Enhancing Signal Space Diversity for SCMA Over Rayleigh Fading Channels

Qu Luo, *Graduate Student Member, IEEE,* Zilong Liu, *Senior Member, IEEE,* Gaojie Chen, *Senior Member, IEEE,* and Pei Xiao, *Senior Member, IEEE.*

Abstract—Sparse code multiple access (SCMA) is a promising technique for the enabling of massive connectivity in future machine-type communication networks, but it suffers from a limited diversity order which is a bottleneck for significant improvement of error performance. This paper aims for enhancing the signal space diversity of sparse code multiple access (SCMA) by introducing quadrature component delay to the transmitted codeword of a downlink SCMA system in Rayleigh fading channels. Such a system is called SSD-SCMA throughout this work. By looking into the average mutual information (AMI) and the pairwise error probability (PEP) of the proposed SSD-SCMA, we develop novel codebooks by maximizing the derived AMI lower bound and a modified minimum product distance (MMPD), respectively. The intrinsic asymptotic relationship between the AMI lower bound and proposed MMPD based codebook designs is revealed. Numerical results show significant error performance improvement in the both uncoded and coded SSD-SCMA systems.

Index Terms—Sparse code multiple access (SCMA), signal space diversity (SSD), average mutual information (AMI), lower bound, modified minimum product distance (MMPD), codebook design.

I. INTRODUCTION

THe widespread proliferation of wireless services and internet-of-thing (IoT) devices is challenging the legacy human-centric mobile networks. For higher spectral efficiency and lower communication latency, there has been a paradigm shift in recent years in the study of non-orthogonal multiple access (NOMA), where the same time/frequency resources are shared for the supporting of several times of more active users [1], [2]. Among many others, this work is concerned with a representative code-domain NOMA (CD-NOMA) technique called sparse code multiple access (SCMA), where multiple users communicate concurrently with distinctive sparse codebooks [3]. At the transmitter, the incoming message bits of each SCMA user are directly mapped to a multi-dimensional sparse codeword drawn from a carefully designed codebook [4], [5]. As pointed out in [1], the conventional SCMA (C-SCMA) suffers from a small diversity order which is a critical bottleneck for fundamental improvement of the SCMA error performance. Therefore, it is pivotal to look for new and affordable SCMA transmission schemes for significant enhancement of its system signal space diversity (SSD).

Qu Luo, Gaojie Chen and Pei Xiao are with 5G & 6G Innovation Centre, Institute for Communication Systems (ICS), University of Surrey, UK, email:{q.u.luo, gaojie.chen, p.xiao}@surrey.ac.uk.

Zilong Liu is with the School of Computer Science and Electronic Engineering, University of Essex, UK, email: zilong.liu@essex.ac.uk.

A. Related Works

SSD, as an effective transmission scheme for higher diversity, has received a sustained research attention in the past decades. A power- and bandwidth-efficient way to acquire SSD was proposed in [6] by coordinate interleaving with constellation rotation. For significant performance gain, the rotation angles of different constellations were investigated in [7], [8] for uncoded systems and in [9], [10] for bit-interleaved coded modulation (BICM) systems. In [11], a different approach to attain full diversity was proposed by judiciously permuting a one-dimensional real-constellation through combinatorial optimization to form a multi-dimensional codebook. This was soon followed by [12] with a low-complexity list-based detection algorithm that works for SSD with both partial- and full-diversity multi-dimensional codebooks. It is noted that the above works [6]–[12] were mainly conducted in a single user system with OMA transmission. As far as multiuser communication is concerned, there have been some works on the exploiting the SSD in power-domain NOMA (PD-NOMA) systems [13]–[17]. In these works, the composite constellations with different rotation angles were obtained for two or more users by optimizing certain criteria such as minimum distance, maximum mutual information (MI), and minimum pairwise error probability (PEP). To the best of our knowledge, however, no results are known on SSD assisted SCMA.

An important aspect of SCMA system optimization is sparse codebook design in order to achieve excellent error rate performances in different channel conditions. Existing codebook designs mainly follow a multi-stage design optimization by first constructing a common multidimensional constellation, called a mother constellation (MC), upon which certain user-specific operations (e.g., interleaving, permutation, shuffling and phase rotations) are applied to the MC to obtain codebooks for multiple users [18]–[22]. In general, the MC and user-specific operations can be designed by minimizing the PEP conditioned to certain channel conditions [18]–[23] or maximizing the system capacity [24]–[28]. By looking into the PEP over Gaussian and Rayleigh fading channels, it is desirable to maximize the minimum Euclidean distance (MED) and minimum product distance (MPD) of a MC or a codebook. Following this spirit, [18] considered Star-QAM as the MC for enlarged MED of the superimposed codewords in downlink SCMA systems. Golden angle modulation (GAM) constellation was adopted in [19] to construct SCMA codebooks with low peak-to-average power ratio properties. In [20],

near-optimal codebooks for different channel conditions were investigated by choosing suitable MCs with large MPD. A uniquely decomposed constellation group based codebook design approach was proposed in [21] by maximizing the MED at each resource node and the MPD of the MC. Downlink quaternary sparse codebook with large MED was obtained in [23] by solving a non-convex optimization problem. Recently, a novel class of low-projection SCMA codebooks for ultra-low decoding complexity was developed in [22] by maximizing the proposed distance metric over Rician fading channels.

SCMA codebooks can also be optimized from the capacity perspective, as shown in [24]–[28]. In [24], a gradient based algorithm was proposed to optimize the average mutual information (AMI), where the AMI was calculated by Monte Carlo method due to the unavailability of its closed form [24]. To avoid the prohibitively high-complexity AMI computation, the cutoff rate was considered in SCMA codebook optimization in [25]–[27]. Specifically, [25] proposed a performance criterion based on the cutoff rate of the equivalent multiple-input multiple-output SCMA system for uplink Rayleigh fading channels. In [26], new MCs were obtained by looking into the constellation constrained sum rate capacity. The cut-off rate combined with constellation shaping gain were considered in [27]. More recently, a novel sparse codebook was obtained in [28] by maximizing the derived lower bound of AMI. However, the lower bound with closed-form of AMI for Rayleigh fading channels is still missing. It is noted that the M-order pulse-amplitude modulation (M-PAM) was employed as the basic constellation in [26]–[28], thus their resultant codebooks exhibit certain similarity.

B. Motivations and Contributions

Against the aforementioned background, the motivations of this work are the two-fold: 1) As SSD can provide enhanced diversity gain over fading channels, a fundamental investigation on the amalgamation of SSD and SCMA, refereed to as SSD-SCMA, is necessary on the theoretical trade-offs and design guidelines; 2) Albeit there are numerous SCMA codebook designs based on PEP or capacity, these codebooks may not be optimal for SSD-SCMA.

The main novelties and contributions of the paper are summarized as follows:

- We introduce quadrature component delay to the superimposed codeword of a downlink SCMA for efficient acquisition of SSD, where the resultant system is called SSD-SCMA. Interestingly, we show that the resultant diversity order is doubled compared to that in conventional SCMA, thus leading to significantly improved reliability in Rayleigh fading channels. To guide the system design, an AMI lower bound and a PEP upper bound are derived.
- Based on the derived AMI lower bound and the modified minimum product distance (MMPD) from the proposed PEP upper bound, we formulate systematic design metrics including the MC design, sparse codebook optimization, and bit labeling from both the PEP and AMI perspectives. In addition, we fill a gap in the current SCMA literature on the asymptotic relationship between PEP and AMI based design metrics, thus bridging the fundamental connection of these two SCMA codebook design techniques.
- We develop an enhanced GAM (E-GAM) as the N-dimensional MC for the proposed AMI based codebooks (AMI-CBs). The joint optimization of MC and rotation angles by maximizing the AMI lower bound are carried out with an interior point method (IPM) with random initial values and Monte Carlo sample estimation. For the proposed PEP based codebooks (P-CBs), we advocate the permutation of a basic one-dimensional constellations that owns large MED to construct the N-dimensional MC. The rotation angles for different users are optimized based on the proposed multi-stage search.
- We conduct extensive numerical experiments to show the superiority of the proposed SSD-SCMA systems and the proposed codebooks in both uncoded and BICM with iterative demapping and decoding (BICM-IDD) systems. The simulations indicate that significant error performance gains are achieved for SSD-SCMA with the proposed AMI-CBs and P-CBs compared to the C-SCMA systems with the state-of-the-art codebooks.

C. Organization

The rest of the paper is organized as follows. In Section II, the system model of downlink SSD-SCMA along with the multiuser detection technique are presented. Section III analyzes the AMI and PEP of the SSD-SCMA system in Rayleigh fading channels. In Section IV, the codebook design problems for SSD-SCMA are formulated in terms of the AMI and PEP. The detailed design of AMI-CB and P-CB is elaborated in Section V. The numerical results are given in Section VI. Finally, conclusions are made in Section VII.

D. Notation

The n-dimensional complex, real and binary vector spaces are denoted as $\mathbb{C}^n$, $\mathbb{R}^n$ and $\mathbb{B}^n$, respectively. Similarly, $\mathbb{C}^{k \times n}$, $\mathbb{R}^{k \times n}$ and $\mathbb{B}^{k \times n}$ denote the $(k \times n)$-dimensional complex, real and binary matrix spaces, respectively. $\mathbf{I}_n$ denotes an $n \times n$-dimensional identity matrix. $\mathrm{tr}(\mathbf{X})$ denotes the trace of a square matrix $\mathbf{X}$. $\mathrm{diag}(\mathbf{x})$ gives a diagonal matrix with the diagonal vector of $\mathbf{x}$. $(\cdot)^{\mathcal{T}}$, $(\cdot)^{\dagger}$ and $(\cdot)^{\mathcal{H}}$ denote the transpose, the conjugate and the Hermitian transpose operation, respectively. $\|\mathbf{x}\|_2$ and $|x|$ return the Euclidean norm of vector $\mathbf{x}$ and the absolute value of x, respectively. $\mathbf{x}_{\mathrm{I}}$ and $\mathbf{x}_{\mathrm{Q}}$ return the in-phase (I) and quadrature (Q) components of the vector, respectively.

II. INTRODUCTION TO THE PROPOSED SSD-SCMA

A. SCMA Communication Model

We consider a downlink SCMA system where J users communicate over K orthogonal resources. The overloading factor, defined as $\lambda = \frac{J}{K}$, is larger than 100%. On the transmitter side, each user maps $\log_2(M)$ binary bits to a length-K codeword $\mathbf{x}_j$ drawn from a pre-defined codebook $\boldsymbol{\mathcal{X}}_j \in \mathbb{C}^{K \times M}$, where M denotes the modulation order. The
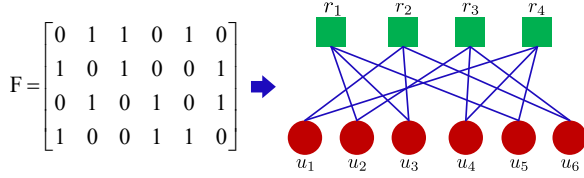
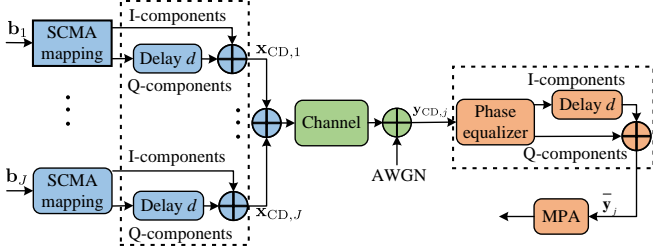Fig. 1: Factor representation of a (4×6) SCMA system.

Fig. 2: Block diagram for the proposed SSD-SCMA system with quadrature component delay in a downlink Rayleigh fading channel.

mapping relationship is expressed as $f_j : \mathbb{B}^{\log_2 M \times 1} \to \mathcal{X}_j \in \mathbb{C}^{K \times M}$, i.e., $\mathbf{x}_j = f_j(\mathbf{b}_j)$, where the codeword set for the jth user is given by $\mathcal{X}_j = \{\mathbf{x}_{j,1}, \mathbf{x}_{j,2}, \ldots, \mathbf{x}_{j,M}\}$ and $\mathbf{b}_j = [b_{j,1}, b_{j,2}, \ldots, b_{j,\log_2 M}]^{\mathcal{T}} \in \mathbb{B}^{\log_2 M \times 1}$ stands for the jth user's instantaneous input binary message vector. The K-dimensional complex codewords in the SCMA codebook are sparse vectors with N non-zero elements and $N < K$. The sparsity of the codebooks enables the low complexity message passing algorithm (MPA) detection at receiver. Let $\mathbf{c}_j$ be a length-N vector drawn from $\mathcal{C}_j \subset \mathbb{C}^{N \times M}$, where $\mathcal{C}_j$ is obtained by removing all the zero elements in $\mathcal{X}_j$. We further define the mapping from $\mathbb{B}^{\log_2 M}$ to $\mathcal{C}_j$ as $g_j : \mathbb{B}^{\log_2 M \times 1} \mapsto \mathcal{C}_j$, i.e., $\mathbf{c}_j = g_j(\mathbf{b}_j)$. The SCMA mapping now can be re-written as

$$f_j :\equiv \mathbf{V}_j g_j, \quad \text{i.e., } \mathbf{x}_j = \mathbf{V}_j g_j(\mathbf{b}_j), \quad (1)$$

where $\mathbf{V}_j \in \mathbb{B}^{K \times N}$ is a mapping matrix that maps the N-dimensional vector to a K-dimensional sparse codewords. The sparse structure of the J SCMA codebooks can be represented by the indicator matrix (factor graph) $\mathbf{F}_{K \times J} = [\mathbf{f}_1, \ldots, \mathbf{f}_J] \subset \mathbb{B}^{K \times J}$ where $\mathbf{f}_j = \text{diag}(\mathbf{V}_j \mathbf{V}_j^{\mathcal{T}})$. An element of $\mathbf{F}$ is defined as $f_{k,j}$ which takes the value of 1 if and only if the user node u_j is connected to resource node r_k and 0 otherwise. Fig. 1 illustrates an SCMA factor graph with $J = 6$, $K = 4$ and $N = 2$.

B. Proposed SSD-SCMA

The key idea of SSD-SCMA is to introduce a delay d for the quadrature component of the SCMA codeword, where the delay time d is assumed to be larger than the channel coherence time [9], [10]. After the component delay (CD), the transmit signal of jth user is represented by $\mathbf{x}_{\text{CD},j}$. The block diagram for the proposed SCMA systems with CD is shown in Fig. 2.

After the CD module, the transmitted vector is obtained by $\mathbf{r}_{\text{CD}} = \sum_{j=1}^{J} \mathbf{x}_{\text{CD},j}$. Accordingly, the received signal at the jth

user can be written as

$$\mathbf{y}_{\text{CD},j} = \text{diag}(\mathbf{h}_{\text{CD},j}) \mathbf{r}_{\text{CD}} + \mathbf{z}_j, \quad (2)$$

where $\mathbf{h}_{\text{CD},j} \in \mathbb{C}^{K \times 1}$ is the channel coefficient vector between the base station and the jth user, and $\mathbf{z}_j \in \mathbb{C}^{K \times 1}$ is the complex additive white Gaussian noise (AWGN) vector with the variance with zero mean and variance N_0. We assume that perfect CSI is available at the receiver. After the phase equalizer, the received signal is transformed into $\frac{\text{diag}(\mathbf{h}_{\text{CD},j}^\dagger)}{|\text{diag}(\mathbf{h}_{\text{CD},j})|} \mathbf{y}_{\text{CD},j} = |\text{diag}(\mathbf{h}_{\text{CD},j})| \mathbf{r}_{\text{CD}} + \frac{\text{diag}(\mathbf{h}_{\text{CD},j}^\dagger)}{|\text{diag}(\mathbf{h}_{\text{CD},j})|} \mathbf{z}_j$ [6]–[12]. Since the noise $\mathbf{z}_j$ is circularly symmetric, $\frac{\text{diag}(\mathbf{h}_{\text{CD},j}^\dagger)}{|\text{diag}(\mathbf{h}_{\text{CD},j})|} \mathbf{z}_j$ has the same distribution of noise $\mathbf{z}_j$. Denote $\bar{\mathbf{y}}_j$ by the received signal after delaying the in-phase component of the received K-dimensional vector. We further let $\mathbf{h}_j^{\text{I}} = [h_{j,1}^{\text{I}}, h_{j,2}^{\text{I}}, \ldots, h_{j,K}^{\text{I}}]^{\mathcal{T}}$ and $\mathbf{h}_j^{\text{Q}} = [h_{j,1}^{\text{Q}}, h_{j,2}^{\text{Q}}, \ldots, h_{j,K}^{\text{Q}}]^{\mathcal{T}}$ be the channel gains associated with the I and Q components of the transmitted vector $\mathbf{r}$, respectively. The elements of $\mathbf{h}_j^{\text{I}}$ and $\mathbf{h}_j^{\text{Q}}$ are Rayleigh distributed independent random variables with zero mean and unit variance. Then, $\bar{\mathbf{y}}_j$ can be demultiplexed into two independent parallel channels [29]:

$$\mathbf{y}_j = \mathbf{H}_j \mathbf{w} + \mathbf{n}_j = \begin{bmatrix} |\text{diag}(\mathbf{h}_j^{\text{I}})| & 0 \\ 0 & |\text{diag}(\mathbf{h}_j^{\text{Q}})| \end{bmatrix} \begin{bmatrix} \mathbf{r}_{\text{I}} \\ \mathbf{r}_{\text{Q}} \end{bmatrix} + \begin{bmatrix} \bar{\mathbf{z}}_{j,\text{I}} \\ \bar{\mathbf{z}}_{j,\text{Q}} \end{bmatrix}, \quad (3)$$

where $\mathbf{y}_j = [\bar{\mathbf{y}}_{j,\text{I}}^{\mathcal{T}}, \bar{\mathbf{y}}_{j,\text{Q}}^{\mathcal{T}}]^{\mathcal{T}} \in \mathbb{R}^{2K \times 1}$, $\mathbf{r} = \sum_{j=1}^{J} \mathbf{x}_j$, and $\mathbf{w} = [\mathbf{r}_{\text{I}}^{\mathcal{T}}, \mathbf{r}_{\text{Q}}^{\mathcal{T}}]^{\mathcal{T}}$. $\mathbf{n}_j = [\bar{\mathbf{z}}_{\text{I}}^{\mathcal{T}}, \bar{\mathbf{z}}_{\text{Q}}^{\mathcal{T}}]^{\mathcal{T}}$ is the real Gaussian noise vector with the variance with zero mean and variance $\frac{N_0}{2}$, and $\bar{\mathbf{z}}_j = \frac{\text{diag}(\mathbf{h}_j^\dagger)}{|\text{diag}(\mathbf{h}_j)|} \mathbf{z}_j$. For simplicity, the subscript j in (3) is omitted whenever no ambiguity arises.

Observed from (3), the I and Q components of the transmitted codewords experience independent Rayleigh fading channels. We will show later that the proposed SSD-SCMA along with efficient codebook design can significantly improve the communication reliability in fading channels.

C. MPA Detection

The received signal $\bar{\mathbf{y}}$ will be inputted into the MPA decoder for efficient multi-user detection. The MPA detector exploits the connections between the user nodes and resource nodes, and passes the belief information alongside the edges of the factor graph. Define the sets $\varphi_j = \{k : f_{j,k} = 1\}$, representing all the resource nodes that user j has active transmission, and $\phi_k = \{j : f_{j,k} = 1\}$, consisting of all the users colliding over resource node k. Following the basic principle of the MPA, at the tth iteration, the belief message propagating from resource node r_k to user node u_j, denoted by $I_{r_k \to u_j}^t(\mathbf{x}_j)$, and the belief message propagating from user node u_j to resource node r_k, denoted by $I_{u_j \to r_k}^{(t)}(\mathbf{x}_j)$, can be expressed respectively as [30]

$$I_{r_k \to u_j}^t(\mathbf{x}_j) = \sum_{\substack{i \in \phi_k \setminus \{j\} \\ \mathbf{x}_i \in \mathcal{X}_i}} p(\bar{y}_k | \mathbf{x}_i) \prod_{i \in \phi_k \setminus \{j\}} I_{u_i \to r_k}^{(t-1)}(\mathbf{x}_i), \quad (4)$$

and

$$I_{u_j \to r_k}^{(t)}(\mathbf{x}) = \alpha_j \prod_{\ell \in \varphi_j \setminus \{k\}} I_{r_\ell \to u_j}^{(t)}(\mathbf{x}), \quad (5)$$

where $\overline{y}_k$ is the kth entry of $\overline{\mathbf{y}}$, α_j is a normalization factor and the probability distribution function of $p\left(\overline{y}_k|\mathbf{x}_i\right)$ is given by

$$p\left(\overline{y}_k|\mathbf{x}_i\right) = \frac{1}{\sqrt{2\pi N_0}} \exp\left(-\frac{\sum_{l\in\{\mathrm{I,Q}\}}\left|\overline{y}_{l,k} - |h_k^l|\sum_{i\in\phi_k} x_{l,k,i}\right|^2}{2N_0}\right).$$

(6)

III. AMI DERIVATION AND ERROR PERFORMANCE ANALYSIS

This section first derives the AMI and its lower bound of the proposed SSD-SCMA system, followed by the error performance analysis based on the PEP.

A. The AMI of the Proposed SSD-SCMA

Let $\boldsymbol{\mathcal{X}} = \{\boldsymbol{\mathcal{X}}_1, \boldsymbol{\mathcal{X}}_2, \ldots, \boldsymbol{\mathcal{X}}_J\}$ denote the J users' sparse codebooks. For the input vector $\mathbf{w}$ given in (3), the AMI of SSD-SCMA is given by [24]

$$\begin{aligned}
\mathcal{I}_{AMI}^{\boldsymbol{\mathcal{X}}} &= \mathcal{H}\left(\mathbf{w}\right) - \mathcal{H}\left(\mathbf{w}|\mathbf{y},\mathbf{H}\right) \\
&= J\log_2(M) - \mathbb{E}_{\mathbf{w},\mathbf{y},\mathbf{H}}\left\{\log_2\frac{\sum_{\hat{\mathbf{w}}\neq\mathbf{w}} p(\mathbf{y}|\hat{\mathbf{w}},\mathbf{H})}{p(\mathbf{y}|\mathbf{w},\mathbf{H})}\right\} \\
&= J\log_2(M) - \frac{1}{M^J}\sum_{m=1}^{M^J}\mathbb{E}_{\mathbf{H},\mathbf{n}}\left\{\log\sum_{p=1}^{M^J}\exp\left(-d_{m,p}\right)\right\},
\end{aligned}$$

(7)

where $\mathcal{H}\left(\mathbf{w}|\mathbf{y},\mathbf{H}\right)$ denotes the entropy of $\mathbf{w}$ conditioned on $\mathbf{H}$ and $\mathbf{y}$, and

$$d_{m,p} = \frac{\|\mathbf{H}\left(\mathbf{w}_p - \mathbf{w}_m\right) + \mathbf{n}\|^2 - \|\mathbf{n}\|^2}{N_0}.$$

(8)

The AMI bounds the maximal information rate of the codebook set $\boldsymbol{\mathcal{X}} = \{\boldsymbol{\mathcal{X}}_1, \boldsymbol{\mathcal{X}}_2, \ldots, \boldsymbol{\mathcal{X}}_J\}$ that can be reliably transmitted with equiprobable inputs. In general, it is challenging to obtain the AMI closed form. As an alternative solution, we deduce the analytical lower bound of AMI to evaluate the transmit efficiency with finite input $\boldsymbol{\mathcal{X}}$.

Lemma 1: The AMI of the SSD-SCMA system in downlink Rayleigh fading channels is upper bounded by

$$\mathcal{I}_{UP}^{\boldsymbol{\mathcal{X}}} = J\log(M) - \sum_{m=1}^{M^J}\log\left(\sum_{p=1}^{M^J}\exp\left(-\frac{\|\mathbf{r}_p - \mathbf{r}_m\|^2}{N_0}\right)\right).$$

(9)

Proof: For given $\mathbf{H}$, we have

$$\begin{aligned}
\mathcal{H}\left(\mathbf{w}|\mathbf{y},\mathbf{H}\right) &\overset{\text{(i)}}{\geq} \sum_{m=1}^{M^J}\log\left(\sum_{p=1}^{M^J}\exp\left(\mathbb{E}_{\mathbf{n}}\left\{-d_{m,p}\right\}\right)\right) \\
&= \sum_{m=1}^{M^J}\log\left(\sum_{p=1}^{M^J}\exp\left(-\frac{\|\mathbf{H}\left(\mathbf{w}_p - \mathbf{w}_m\right)\|^2}{N_0}\right)\right),
\end{aligned}$$

(10)

where (i) is obtained by applying Jensen's inequality since the log-sum-exp function is a convex function of $d_{m,p}$. Upon

taking expectation of $\mathbf{H}$ on both sides of (10), we have

$$\begin{aligned}
\mathcal{H}\left(\mathbf{w}|\mathbf{y}\right) &= \mathbb{E}_{\mathbf{H}}\left\{\mathcal{H}\left(\mathbf{w}|\mathbf{y},\mathbf{H}\right)\right\} \\
&\overset{\text{(ii)}}{\geq} \sum_{m=1}^{M^J}\log\left(\sum_{p=1}^{M^J}\exp\left(\mathbb{E}_{\mathbf{H}}\left\{-\frac{\|\mathbf{H}\left(\mathbf{w}_p - \mathbf{w}_m\right)\|^2}{N_0}\right\}\right)\right) \\
&= \sum_{m=1}^{M^J}\log\left(\sum_{p=1}^{M^J}\exp\left(-\frac{\|\left(\mathbf{r}_p - \mathbf{r}_m\right)\|^2}{N_0}\right)\right).
\end{aligned}$$

(11)

Substituting (11) into

$$\mathcal{I}(\mathbf{w};\mathbf{y}) = J\log_2(M) - \mathbb{E}_{\mathbf{H}}\left\{\mathcal{H}\left(\mathbf{w}|\mathbf{y},\mathbf{H}\right)\right\}$$

(12)

yields the upper bound in (9).

Lemma 2: The AMI of the SSD-SCMA system in downlink Rayleigh fading channels is lower bounded by

$$\mathcal{I}_{LB}^{\boldsymbol{\mathcal{X}}} = 2J\log(M) - K\left(\frac{1}{\ln 2} - 1\right) - \log\left(\sum_{m=1}^{M^J}\sum_{p=1}^{M^J}\prod_{k=1}^{K}\gamma_{k,m,p}\right),$$

(13)

where

$$\gamma_{k,m,p} = \prod_{l\in\{\mathrm{I,Q}\}}\left(1 + \frac{\left|\sum_{j\in\phi_k} x_{j,m,l}[k] - x_{j,p,l}[k]\right|^2}{4N_0}\right)^{-1}.$$

(14)

Proof: By taking the noise term $\frac{\|\mathbf{n}\|^2}{N_0}$ in $d_{m,p}$ out the summation, we can reformulate the $\mathcal{H}\left(\mathbf{w}|\mathbf{y},\mathbf{H}\right)$ in (7) as [31]

$$\begin{aligned}
&\mathcal{H}\left(\mathbf{w}|\mathbf{y},\mathbf{H}\right) \\
&= \mathbb{E}_{\mathbf{n}}\log\exp(\frac{\|\mathbf{n}\|^2}{N_0}) + \frac{1}{M^J}\sum_{m=1}^{M^J}\mathbb{E}_{\mathbf{n}}\left\{\log\sum_{p=1}^{M^J}\exp\left(e_{m,p}\right)\right\} \\
&\overset{\text{(i)}}{\leq} \frac{K}{\ln 2} + \log\left(\frac{1}{M^J}\sum_{m=1}^{M^J}\sum_{p=1}^{M^J}\mathbb{E}_{\mathbf{n}}\left\{\exp\left(e_{m,p}\right)\right\}\right),
\end{aligned}$$

(15)

where $e_{m,p} = -\frac{\|\mathbf{H}(\mathbf{w}_p - \mathbf{w}_m) + \mathbf{n}\|^2}{N_0}$. Considering the integral interval of $(-\infty,\infty)$ for the second term of the right-hand side, we have $\mathbb{E}_{\mathbf{n}}\left\{\log\exp(\|\mathbf{n}\|^2/N_0)\right\} = \frac{K}{\ln 2}$. Since $\log(x)$ is a concave function, a lower bound for the AMI in (15) is derived by applying Jensen's inequality, i.e., step (i). The expectation over $\mathbf{n}$ in (15) is given by

$$\begin{aligned}
&\mathbb{E}_{\mathbf{n}}\left\{\exp\left(e_{m,p}\right)\right\} \\
&= \int \frac{1}{(\pi N_0)^K}\exp\left(\frac{-\|\mathbf{n}\|^2}{N_0}\right)\exp\left(e_{m,p}\right)\mathrm{d}\mathbf{n} \\
&= \prod_{k=1}^{2K}\frac{1}{(\pi N_0)^K}\int_{n_k}\exp\left(-\frac{|n_k + |h_k|\left(w_{p,k} - w_{m,k}\right)|^2 + |n_k|^2}{N_0}\right)\mathrm{d}n_k \\
&\overset{\text{(i)}}{=} \frac{1}{2^K}\prod_{k=1}^{2K}\exp\left(-\frac{|h_k|^2\delta_{p,m,k}^2}{2N_0}\right),
\end{aligned}$$

(16)

where step (i) is derived based on the (2.33.1) in [32], $\delta_{p,m,k}^2 = (w_{p,k} - w_{m,k})^2$, $|h_k|$ is the kth entry of diag($\mathbf{H}$), and $w_{m,k}$ is the kth entry of $\mathbf{w}_m$. Then, substituting (16) into (15) and

taking expectation of $\mathbf{H}$ on the both sides, we obtain

$$\mathcal{H}\left(\mathbf{w}|\mathbf{y}\right) = \mathbb{E}_{\mathbf{H}}\left\{\mathcal{H}\left(\mathbf{w}|\mathbf{y},\mathbf{H}\right)\right\}$$

$$\leq \frac{K}{\ln 2} - J\log(M)$$

$$+ \mathbb{E}_{\mathbf{H}}\left\{\log\left(\sum_{m=1}^{M^J}\sum_{p=1}^{M^J}\frac{1}{2^K}\prod_{k=1}^{2K}\exp\left(-\frac{|h_k|^2\delta_{p,m,k}^2}{2N_0}\right)\right)\right\}$$

$$\leq K\left(\frac{1}{\ln 2} - 1\right) - J\log(M)$$

$$+ \log\left(\sum_{m=1}^{M^J}\sum_{p=1}^{M^J}\prod_{k=1}^{2K}\mathbb{E}_{\mathbf{H}}\left\{\exp\left(-\frac{|h_k|^2\delta_{p,m,k}^2}{4N_0}\right)\right\}\right)$$

$$\stackrel{(i)}{=} K\left(\frac{1}{\ln 2} - 1\right) - J\log(M)$$

$$+ \log\left(\sum_{m=1}^{M^J}\sum_{p=1}^{M^J}\prod_{k=1}^{K}\prod_{l\in\{I,Q\}}\left(1+\frac{\left|\sum_{j\phi_k}x_{j,m,l}[k]-x_{j,p,l}[k]\right|^2}{4N_0}\right)^{-1}\right),$$

(17)

where step (i) is obtained base on the fact that the $s = h_k^2$ has a chi-square probability distribution with its moment generating function, which is defined as $\mathbb{E}\left[e^{-st}\right]$, given by $M_s(t) = \frac{1}{1+t}$. Substituting (17) into (12) leads to the lower bound in (13).

Remark 1: Following a similar derivation to the above for Lemma 2, we can obtain the lower bound of AMI for conventional SCMA, which has the same form from (13), but with different expression of $\gamma_{k,m,p}$ given by

$$\gamma_{k,m,p} = \left(1+\frac{\left|\sum_{j\in\phi_k}x_{j,m}[k]-x_{j,p}[k]\right|^2}{4N_0}\right)^{-1}. \quad (18)$$

Remark 2: For $N_0 \to 0$ and $N_0 \to \infty$, $\mathcal{I}_{LB}$ approaches to $-K\left(1/\ln 2 - 1\right)$ and $J\log M - K\left(1/\ln 2 - 1\right)$, respectively. This indicates that at low and high signal-to-noise ratio (SNR) regions, there exists a constant gap $-K\left(1/\ln 2 - 1\right)$ between $\mathcal{I}_{LB}$ and $\mathcal{I}_{AMI}^{\mathcal{X}}$. The lower bound with a constant shift can well approximate the AMI, particularly in the low and high SNR regions. In medium SNR region, the gap between the lower bound and AMI is intractable. In fact, maximizing the lower bound is still an efficient approach to improve the AMI in the medium SNR region [28], [31].

B. Error Performance Analysis of the Proposed SSD-SCMA

Assume that the erroneously decoded codeword is $\hat{\mathbf{w}}$ when $\mathbf{w}$ is transmitted, where $\hat{\mathbf{w}} \neq \mathbf{w}$. Furthermore, let us define the element-wise distance $\tau_{\mathbf{w}\to\hat{\mathbf{w}}}(k) = |w_k - \hat{w}_k|^2$ [1]. Then, the pairwise-error probability conditioned on the channel fading vector for a maximum-likelihood receiver is given as [1]

$$\Pr\{\mathbf{w}\to\hat{\mathbf{w}}|\mathbf{H}\} = Q\left(\sqrt{\frac{\sum_{k=1}^{2K}h_k^2\tau_{\mathbf{w}\to\hat{\mathbf{w}}}(k)}{2N_0}}\right), \quad (19)$$

where $Q(t) = \frac{1}{\pi}\int_0^{+\infty}\frac{e^{-\frac{x^2}{2}(t^2+1)}}{t^2+1}dt$ is the Gaussian Q-function [33]. By letting $\gamma_{\mathbf{w}\to\hat{\mathbf{w}}}(k) = \tau_{\mathbf{w}\to\hat{\mathbf{w}}}(k)/4N_0$ and with

the expectation over the channel vector, one has

$$\Pr\{\mathbf{w}\to\hat{\mathbf{w}}\}$$

$$= \frac{1}{\pi}\int_0^{+\infty}\frac{\mathbb{E}_{\mathbf{H}}\left\{\exp\left\{-(t^2+1)\sum_{k=1}^{2K}h_k^2\gamma_{\mathbf{w}\to\hat{\mathbf{w}}}(k)\right\}\right\}}{t^2+1}dt \quad (20)$$

$$= \frac{1}{\pi}\int_0^{+\infty}\frac{1}{t^2+1}\prod_{k=1}^{2K}\frac{1}{1+\gamma_{\mathbf{w}\to\hat{\mathbf{w}}}(k)(t^2+1)}dt.$$

To proceed, define the set $\eta_{\mathbf{w}\to\hat{\mathbf{w}}} \triangleq \{k : \tau_{\mathbf{w}\to\hat{\mathbf{w}}}(k) \neq 0, 1 \leq k \leq 2K\}$, and let $G_{\mathbf{w}\to\hat{\mathbf{w}}}$ be the cardinality of $\eta_{\mathbf{w}\to\hat{\mathbf{w}}}$. We further define $\delta_k \triangleq \frac{\gamma_{\mathbf{w}\to\hat{\mathbf{w}}}(k)}{1+\gamma_{\mathbf{w}\to\hat{\mathbf{w}}}(k)}$ and $\delta_{\min} = \min\{\delta_k : k \in \eta_{\mathbf{w}\to\hat{\mathbf{w}}}\}$. Thus, the PEP can be written as [34]

$$\Pr\{\mathbf{w}\to\hat{\mathbf{w}}\} \leq B(G_{\mathbf{w}\to\hat{\mathbf{w}}},\delta_{\min})\prod_{k=1}^{2K}\frac{1}{1+\gamma_{\mathbf{w}\to\hat{\mathbf{w}}}(k)^2}, \quad (21)$$

where

$$B(G_{\mathbf{w}\to\hat{\mathbf{w}}},\delta_{\min})$$

$$= \frac{1}{4^{G_{\mathbf{w}\to\hat{\mathbf{w}}}}}\sum_{l=0}^{G_{\mathbf{w}\to\hat{\mathbf{w}}}-1}\binom{G_{\mathbf{w}\to\hat{\mathbf{w}}}-1+l}{G_{\mathbf{w}\to\hat{\mathbf{w}}}}\left(\frac{2}{1+\delta_{\min}}\right)^{G_{\mathbf{w}\to\hat{\mathbf{w}}}-l}. \quad (22)$$

Note that under the asymptotic condition $N_0 \to 0$, (21) is tighter than the Chernoff bound[1] by the factor $B(G_{\mathbf{w}\to\hat{\mathbf{w}}},\delta_{\min})$.

Diversity order: At sufficiently large SNR, since $\gamma_{\mathbf{w}\to\hat{\mathbf{w}}}(k) \to \infty$, thus $\delta_{\min} \approx 1$ and it follows that

$$B(G_{\mathbf{w}\to\hat{\mathbf{w}}},\delta_{\min}) \leq \frac{1}{4^{G_{\mathbf{w}\to\hat{\mathbf{w}}}}}\binom{2G_{\mathbf{w}\to\hat{\mathbf{w}}}-1}{G_{\mathbf{w}\to\hat{\mathbf{w}}}}. \quad (23)$$

Hence, one can approximate the right-hand side of (21) as

$$\Pr\{\mathbf{w}\to\hat{\mathbf{w}}\} \leq G_c\left(\mathbf{w}\to\hat{\mathbf{w}}\right)N_0^{G_d(\mathbf{w}\to\hat{\mathbf{w}})}, \quad (24)$$

where

$$G_c(\mathbf{w}\to\hat{\mathbf{w}}) = \binom{2G_{\mathbf{w}\to\hat{\mathbf{w}}}-1}{G_{\mathbf{w}\to\hat{\mathbf{w}}}}\prod_{k\in\eta_{\mathbf{w}\to\hat{\mathbf{w}}}}|\tau_{\mathbf{w}\to\hat{\mathbf{w}}}(k)|^{-2}. \quad (25)$$

From (24) and (25), define the diversity order (DO) of the SSD-SCMA system as $G_d \triangleq \min_{\mathbf{w}\neq\hat{\mathbf{w}}}G_d(\mathbf{w}\to\hat{\mathbf{w}})$ and the coding gain as $G_c \triangleq \min_{\mathbf{w}\neq\hat{\mathbf{w}},G_d(\mathbf{w}\to\hat{\mathbf{w}})=G_d}G_c(\mathbf{w}\to\hat{\mathbf{w}})$ [35]. The union bound of average bit error rate (ABER) for SSD-SCMA system is given as

$$P_{\mathrm{b}} \leq \frac{1}{M^J \cdot J\log_2(M)}\sum_{\mathbf{w}}\sum_{\hat{\mathbf{w}}\neq\mathbf{w}}n_{\mathrm{E}}(\mathbf{w},\hat{\mathbf{w}}) \cdot \Pr\{\mathbf{w}\to\hat{\mathbf{w}}\}. \quad (26)$$

where $n_e\left(\mathbf{w},\hat{\mathbf{w}}\right)$ is the Hamming distance between $\mathbf{w}$ and $\hat{\mathbf{w}}$. Based on (24) and (26), we introduce the following lemma:

Lemma 3: The proposed SSD-SCMA enjoys maximum DO of $G_d = 2N$, whereas a C-SCMA system only attains DO of at most $G_d = N$.

Proof: In general, the maximum PEP among all code-word pairs dominates the ABER at high SNR values which corresponds to the nearest neighbours among the multi-user codeword pairs. In other words, $G_d(\mathbf{w}\to\hat{\mathbf{w}}) = G_d$ holds for the single error event that all the codewords are detected

---

[1]The Chernoff bound can be obtained by applying $B(G_{\mathbf{w}\to\hat{\mathbf{w}}},\delta_{\min}) = \frac{1}{2}$.

correctly except for a codeword of only one user. Hence, the proposed SSD-SCMA system can achieve maximum DO of $2N$. Specifically, the diversity comes from the following two aspects: whilst the non-zero elements of the sparse codebooks provide a diversity of N (same as the traditional SCMA), the delay in the I/Q component attributes to a diversity increase of two times.

Remark 3: The proposed SSD-SCMA with a DO of $2N$ generally enjoys improved error performance with steeper ABER slope against SNR, compared to C-SCMA system. Observed from (24) and (26), it is ideal to maximize the DO and coding gain of a codebook to improve ABER. In addition, the PEP is also dependent on the element-wise distance $\tau_{\mathbf{w} \to \hat{\mathbf{w}}}(k)$, hence it is also desirable to improve $\tau_{\mathbf{w} \to \hat{\mathbf{w}}}(k)$ for improved ABER.

IV. MULTIDIMENSIONAL CODEBOOK DESIGN: DESIGN METRICS

In this section, we formulate the codebook design metrics according to the AMI and PEP analysis. The main idea is to maximize the lower bound of AMI or minimize the upper bound of PEP.

A. AMI-CB Design by Maximizing the Lower Bound of AMI

Our optimization goal is to maximize the AMI lower bound derived in Lemma 2. Thus, we formulate the codebook design of the SSD-SCMA system with structure of $\mathcal{S}(\mathcal{V}, \mathcal{G}; J, M, N, K)$, $\mathcal{V} := [\mathbf{V}_j]_{j=1}^J$ and $\mathcal{G} := [g_j]_{j=1}^J$ in downlink Rayleigh fading channels as follows:

$$\mathcal{P}_1 : \mathcal{V}^*, \mathcal{G}^* = \arg\max_{\mathcal{V},\mathcal{G}} \quad \mathcal{I}_{LB}^{\boldsymbol{\mathcal{X}}} \tag{27}$$

$$\text{Subject to} \quad \sum_{j=1}^J \text{Tr}\left(\boldsymbol{\mathcal{X}}_j^H \boldsymbol{\mathcal{X}}_j\right) = MJ. \tag{27a}$$

1) MC figure of merit: In general, users' sparse codebooks $\boldsymbol{\mathcal{X}}_j, j = 1, 2, \ldots, J$ are generated from a common MC, denoted as $\boldsymbol{\mathcal{C}}_{MC} \in \mathbb{C}^{N \times M}$, thus the design of MC is crucial. The MC based MI (MC-MI) determines the maximum information rate that can be reliably transmitted for a single user. Naturally, we target maximizing the AMI lower bound of the MC, which can be expressed as

$$\mathcal{I}_{LB}^{\boldsymbol{\mathcal{C}}_{MC}} = \log_2(M) - \frac{N}{\ln 2}$$
$$- \frac{1}{M} \log \left(\sum_{m=1}^M \sum_{p=1}^M \prod_{n=1}^N \left(1 + \frac{|c_{m,n} - c_{p,n}|^2}{4N_0} \right)^{-1} \right), \tag{28}$$

where $c_{m,n}$ is the mth codeword at the nth entry of $\boldsymbol{\mathcal{C}}_{MC}$. Hence, in Rayleigh fading channels, we choose the following cost function for MC design:

$$\mathfrak{G}_j = \sum_{m=1}^M \sum_{p=1}^M \prod_{n=1}^N \left(1 + \frac{\| c_{m,n} - c_{p,n} \|^2}{4N_0} \right)^{-1}. \tag{29}$$

2) Labeling figure of merit: Labeling is crucial for BICM-IDD system. The effect of mapping on the performance of

SSD-SCMA in BICM-IDD systems can be characterized by the simplified criterion [36], [37]:

$$\Upsilon_{\text{Ray}} = \frac{1}{mM} \sum_{i=1}^m \sum_{b=0}^1 \sum_{\mathbf{x} \in \mathcal{X}_i^b} \prod_{k=1}^K \left\{ \frac{1}{1 + \frac{1}{4N_0}|\Re\mathfrak{e}\left(x_k - \hat{x}_k\right)|^2} \right.$$
$$\left. \times \frac{1}{1 + \frac{1}{4N_0}|\Im\mathfrak{m}\left(x_k - \hat{x}_k\right)|^2} \right\}, \tag{30}$$

where $\mathcal{X}_i^b$ denotes the set of codewords that with bit b at ith position. Note that (30) is employed as the cost function to design the labeling for the AMI-CBs.

B. P-CB Design by Minimizing the Upper Bound of PEP

According to the *Remark 3* in Subsection III-B, the ABER is dominated by the DO and the coding gain, i.e., G_c. The DO of user j is given by

$$\text{DO}(\boldsymbol{\mathcal{X}}_j) = \sum_{k=1}^K \text{Ind}\left(|\Re\mathfrak{e}\left(x_{n,i} - x_{n,l}\right)|\right)$$
$$+ \sum_{k=1}^K \text{Ind}\left(|\Im\mathfrak{m}\left(x_{n,i} - x_{n,l}\right)|\right), \tag{31}$$

where $\text{Ind}(x)$ takes the value of one if x is nonzero and zero otherwise. We now formulate the design metric by maximizing the coding gain. For any arbitrary $\mathbf{w}$ and $\hat{\mathbf{w}}$ that $\min_{\mathbf{w} \neq \hat{\mathbf{w}}} G_d(\mathbf{w} \to \hat{\mathbf{w}}) = G_d$, the term $\prod_{k \in \eta_{\mathbf{w} \to \hat{\mathbf{w}}}} |\tau_{\mathbf{w} \to \hat{\mathbf{w}}}(k)|^{-2}$ in (25) equals to the product distance of a single user [1]. To proceed, let us define the modified MPD (MMPD) of the jth user as

$$d_{\text{MMPD}}^{\boldsymbol{\mathcal{X}}_j} = \min_{i \neq l, 1 < i,l < M} d_{\text{P},i,l}^{\boldsymbol{\mathcal{X}}_j}$$
$$= \min_{i \neq l, 1 < i,l < M} \prod_{n \in \rho_1(\mathbf{x}_i, \mathbf{x}_l)} \left\{ |\Re\mathfrak{e}\left(x_{n,i} - x_{n,l}\right)|^2 \right.$$
$$\left. \times \prod_{n \in \rho_2(\mathbf{x}_i, \mathbf{x}_l)} |\Im\mathfrak{m}\left(x_{n,i} - x_{n,l}\right)|^2 \right\}, \tag{32}$$

where $\rho_1(\mathbf{x}_i, \mathbf{x}_l)$ and $\rho_2(\mathbf{x}_i, \mathbf{x}_l)$ denote the sets of indices in which $\Re\mathfrak{e}(x_{n,i}) \neq \Re\mathfrak{e}(x_{n,j})$ and $\Im\mathfrak{m}(x_{n,i}) \neq \Im\mathfrak{m}(x_{n,j})$, respectively. Note that the product distance of one user may be different from that of another due to different user constellation operators. Hence, it is interesting to minimize the MMPD of all users, which is expressed as

$$d_{\text{MMPD}}^{\boldsymbol{\mathcal{X}}} = \min_{j=1,2,\ldots,J} d_{\text{MMPD}}^{\boldsymbol{\mathcal{X}}_j}. \tag{33}$$

Obviously, improving the G_c of a codebook is equivalent to maximizing the $d_{\text{MMPD}}^{\boldsymbol{\mathcal{X}}}$. In addition, we further define the minimum element-wise distance $\tau_{\min}^{\boldsymbol{\mathcal{X}}}$ as

$$\tau_{\min}^{\boldsymbol{\mathcal{X}}} = \min \left\{ \tau_{\mathbf{w} \to \hat{\mathbf{w}}}^2(k) \right.$$
$$\left. |\forall \mathbf{w}_n, \mathbf{w}_m \in \Phi, \mathbf{w}_n \neq \mathbf{w}_m, 1 \leq k \leq 2K \right\}. \tag{34}$$

Based on the *Remark 3* in Subsection III-B, it is desirable to design codebooks to achieve full DO, large MMPD and large $\tau_{\min}^{\boldsymbol{\mathcal{X}}}$. Hence, the codebook design problem of SSD-SCMA is

formulated as

$$\mathcal{P}_{2-1} : \mathcal{V}^*, \mathcal{G}^* = \arg\max_{\mathcal{V}, \mathcal{G}} \left\{ d^{\boldsymbol{\mathcal{X}}}_{\mathrm{MMPD}}, \tau^{\boldsymbol{\mathcal{X}}}_{\min} \right\} \qquad (35)$$

$$\text{Subject to} \quad \mathrm{DO}(\boldsymbol{\mathcal{X}}_j) = 2N, j = 1, 2, \ldots, J, \qquad (35a)$$

$$\sum_{j=1}^{J} \mathrm{Tr}\left(\boldsymbol{\mathcal{X}}_j^H \boldsymbol{\mathcal{X}}_j \right) = MJ. \qquad (35b)$$

1) MC figure of merit:

Similar to the case of MI aided MC design, the MC constrained PEP is employed to guide the design of MC. Specifically, the MC design is formulated as

$$\boldsymbol{\mathcal{C}}^*_{MC} = \max \ \underbrace{\min_{i \neq l} \prod_{n \in \rho(\mathbf{c}_i, \mathbf{c}_l)} |c_{n,i} - c_{n,l}|^2,}_{d^{\boldsymbol{\mathcal{C}}_{MC}}_{\mathrm{MPD}}} \qquad (36)$$

$$\text{Subject to} \quad \begin{matrix} \mathrm{Tr}\left(\boldsymbol{\mathcal{C}}_{MC}^H \boldsymbol{\mathcal{C}}_{MC} \right) = NM, \\ |\rho(\mathbf{c}_i, \mathbf{c}_j)| = N, \end{matrix}$$

where $\rho(\mathbf{c}_i, \mathbf{c}_j)$ denotes the set of indices in which $c_{n,i} \neq c_{n,j}$, and $d^{\boldsymbol{\mathcal{C}}_{MC}}_{\mathrm{MPD}}$ is the MPD of $\boldsymbol{\mathcal{C}}_{MC}$. The rationale for employing $d^{\boldsymbol{\mathcal{C}}_{MC}}_{\mathrm{MPD}}$ is that a MC with large $d^{\boldsymbol{\mathcal{C}}_{MC}}_{\mathrm{MPD}}$ can also enlarge $d^{\boldsymbol{\mathcal{X}}_j}_{\mathrm{MMPD}}$ after applying user-specific operation, such as phase rotation. In addition, it is well known that improving $d^{\boldsymbol{\mathcal{C}}_{MC}}_{\mathrm{MPD}}$ can also improve the ABER of a C-SCMA system.

2) Labeling figure of merit: The labeling rules should be designed to minimize the MC constrained PEP. Under Rayleigh fading channels, the labeling metric is given as [20]

$$\Pi_{\mathbf{R}}(\xi_l) \equiv \sum_{i=1}^{M-1} \sum_{l=i+1}^{M} N_{i,l}(\xi_l) \frac{1}{d^{\boldsymbol{\mathcal{X}}_j}_{\mathrm{P},i,l}}, \qquad (37)$$

where $N_{i,l}(\xi_j)$ denotes the number of different labelling bits between $\mathbf{x}_{j,i}$ and $\mathbf{x}_{j,l}$ based on the considered labelling rule ξ_j.

C. Asymptotic Relationship Between the P-CB and AMI-CB

First, let us look at the AMI lower bound, i.e., $\mathcal{I}^{\boldsymbol{\mathcal{X}}}_{LB}$ in (13), whose value depends on $\sum_{m=1}^{M^J} \sum_{p=1}^{M^J} \prod_{k=1}^{K} \lambda_{k,m,p}$. For sufficiently high SNR, we have

$$\gamma_{k,m,p} \approx \prod_{l \in \{\mathrm{I}, \mathrm{Q}\}} \left(\frac{\left| \sum_{j \in \phi_k} x_{j,m,l}[k] - x_{j,p,l}[k] \right|^2}{4N_0} \right)^{-1}. \qquad (38)$$

The term $\sum_{m=1}^{M^J} \sum_{p=1}^{M^J} \prod_{k=1}^{K} \gamma_{k,m,p}$ is dominated by the most significant term. Thus, for $N_0 \to 0$, we have the following lower bound:

$$\sum_{m=1}^{M^J} \sum_{p=1}^{M^J} \prod_{k=1}^{K} \gamma_{k,m,p} \geq \max_{1 \leq m,p \leq M^J} \ \frac{1}{M^J} \prod_{k=1}^{K} \gamma_{k,m,p}. \qquad (39)$$

It is noted that the right-hand side of (39) essentially corresponds to the MMPD of the codebook, i.e., the $d^{\boldsymbol{\mathcal{X}}}_{\mathrm{MMPD}}$ in (33). Hence, maximizing $\mathcal{I}^{\boldsymbol{\mathcal{X}}}_{LB}$ of a codebook is equivalent to maximizing the $d^{\boldsymbol{\mathcal{X}}}_{\mathrm{MMPD}}$ of codebook at a sufficiently high SNR value.

Remark 4 : Similar results can be obtained for C-SCMA system. Namely, a codebook with larger MPD will result in a higher $\mathcal{I}^{\boldsymbol{\mathcal{X}}}_{LB}$ with $\gamma_{k,m,p}$ given in (18) at a sufficiently high SNR values.

V. MULTIDIMENSIONAL CODEBOOK DESIGN: IMPLEMENTATION ISSUES

This section presents the detailed sparse codebook design for SSD-SCMA based on the proposed design metrics in Section IV. Specifically, Subsection V-A first introduces a constellation superposition scheme, which generates multiple sparse codebooks based on the MC. Then, we present the solutions for $\mathcal{P}_{1-1}$ and $\mathcal{P}_{1-2}$, i.e., (27) and (35), in Subsections V-B and V-C, respectively.

A. Constellation Superposition Scheme

As mentioned, multiple sparse codebooks are generated from a common MC ($\boldsymbol{\mathcal{C}}_{MC} \in \mathbb{C}^{N \times M}$) by user-specific operations. The detail design of $\boldsymbol{\mathcal{C}}_{MC}$ will be discussed later. Once $\boldsymbol{\mathcal{C}}_{MC}$ is determined, phase rotations are applied to design the multi-dimensional constellations for different users. Therefore, the jth user's codebook with non-zero elements is generated as $\boldsymbol{\mathcal{C}}_j = \mathbf{R}_j \boldsymbol{\mathcal{C}}_{MC}$, where $\mathbf{R}_j$ denotes the diagonal phase rotation matrix of the jth user. For example, for an $\boldsymbol{\mathcal{C}}_{MC}$ with $N = 2$, we have $\mathbf{R}_j = \begin{bmatrix} e^{j\theta_1} & 0 \\ 0 & e^{j\theta_2} \end{bmatrix}$. Based on the mapping matrix $\mathbf{V}_j$, the jth user's codebook now can be generated by $\boldsymbol{\mathcal{X}}_j = \mathbf{V}_j \mathbf{R}_j \boldsymbol{\mathcal{C}}_{MC}$. $\mathbf{V}_j$ can be constructed based on the j-th column of $\mathbf{F}$. Specifically, according to the positions of the '0' elements of $\mathbf{f}_j$, we insert the all-zero row vectors into the identity matrix $\mathbf{I}_N$. For example, for the $\mathbf{F}$ in Fig. 1, we have

$$\mathbf{V}_1 = \begin{bmatrix} 0 & 0 \\ 1 & 0 \\ 0 & 0 \\ 0 & 1 \end{bmatrix}, \mathbf{V}_2 = \begin{bmatrix} 1 & 0 \\ 0 & 0 \\ 0 & 1 \\ 0 & 0 \end{bmatrix}. \qquad (40)$$

It is noted that the phase rotation matrix $\mathbf{R}_j$ and the mapping matrix $\mathbf{V}_j$ can be combined together by a column vector, i.e., $\mathbf{s}^j_{N \times J} = \mathbf{V}_j \mathbf{R}_j \mathbf{I}_K$, where $\mathbf{I}_K$ denotes all-one vector of length K. Hence, the codebooks for the J users can be represented by the signature matrix $\mathbf{S}_{N \times J} = \left[\mathbf{s}^1_{N \times J}, \mathbf{s}^2_{N \times J}, \ldots, \mathbf{s}^J_{N \times J} \right]$. In this paper, we consider the following signature matrix:

$$\mathbf{S}_{4 \times 6} = \begin{bmatrix} 0 & e^{j\theta_3} & e^{j\theta_1} & 0 & e^{j\theta_2} & 0 \\ e^{j\theta_2} & 0 & e^{j\theta_3} & 0 & 0 & e^{j\theta_1} \\ 0 & e^{j\theta_2} & 0 & e^{j\theta_1} & 0 & e^{j\theta_3} \\ e^{j\theta_1} & 0 & 0 & e^{j\theta_2} & e^{j\theta_3} & 0 \end{bmatrix}. \qquad (41)$$

B. Design of AMI-CB

1) Proposed Design of $\boldsymbol{\mathcal{C}}_{MC}$: GAM is a novel, shape-versatile and circular symmetric modulation scheme which can offer enhanced MI performance over pulse-amplitude modulation and square quadrature amplitude modulation (QAM) design. This motivates us to employ GAM as the basic MC to design the AMI-CBs. In an N_p-point disc-shaped GAM, the nth constellation point can be generated according to $a_n = r_n e^{i2\pi\varphi n}$, where $r_n = c_{\mathrm{norm}}\sqrt{n}$, $c_{\mathrm{norm}} = \sqrt{\frac{2P}{N_p+1}}$, P is the power constraint and $\varphi = \frac{1-\sqrt{5}}{2}$ is the golden angle in rads. The (ξ, ψ)-GAM is defined as $a_n = c_{\mathrm{norm}}\sqrt{n + \xi}e^{i2\pi(\varphi+\psi)n}$ [19], where ξ and ψ are the two parameters to be optimized in
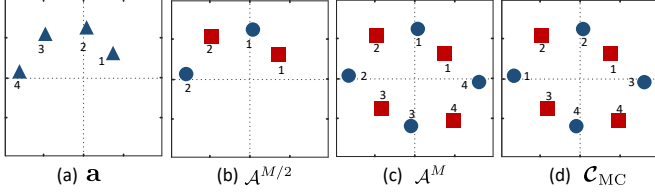
Fig. 3: An MC example based on GAM, where $\xi = 1$, $\psi = -0.74$, $M = 4$, $N = 2$. The elements in (a) are the original GAM points, i.e., $\mathbf{a}$. Subfigures (b) to (d) show the mapping process from $\mathbf{a}$ to $\mathcal{C}_{MC}$. Square and circular marks are the elements of the first and second dimensions, respectively.

Algorithm 1 Design $\mathcal{C}_{MC}$ based on GAM.

Input: ξ, ψ, N, M and N_0

1: **Step 1. Generate the basic constellation**
2: $\mathbf{a} \leftarrow$ Generate $a_l = c_{\text{norm}}\sqrt{l + \xi}e^{i2\pi(\varphi + \psi)L}$, $l = 1, 2, \ldots, \frac{MN}{2}$
3: **for** $l = 1 : \frac{MN}{2}$ **do**
4: $\quad n = \text{mod}(l, N)$
5: $\quad \mathcal{A}^{\frac{M}{2}} \leftarrow$ map the lth element of $\mathbf{a}$ to the nth dimension of $\mathcal{A}^{\frac{M}{2}}$
6: **end for**
7: $\mathcal{A}^M \leftarrow \left(\mathcal{A}^{\frac{M}{2}}, -\mathcal{A}^{\frac{M}{2}} \right)$
8: **Step 2. Dimension permutation**
9: $\mathcal{C}_{MC} \leftarrow \left[\pi_1 \left(\mathcal{A}_1^M \right), \pi_2 \left(\mathcal{A}_2^M \right), \ldots, \pi_N \left(\mathcal{A}_N^M \right) \right]^{\mathcal{T}}$ based on the criteria given in (29)
10: **Step 3. Dimension switching**
11: $\mathcal{C}'_{MC} = \left[\mathbf{c}_N^{\mathcal{T}}, \mathbf{c}_{N-1}^{\mathcal{T}}, \ldots, \mathbf{c}_1^{\mathcal{T}} \right]^{\mathcal{T}}$

---

the MC. Here, we propose an enhanced scheme to construct the MC based on GAM, termed as E-GAM. The design scheme mainly includes the following three steps and the detailed process is given in **Algorithm 1**.

Step 1. Generate the N-dimensional constellation based on GAM, denoted as $\mathcal{A}^M = [\mathbf{a}_1^{\mathcal{T}}, \mathbf{a}_2^{\mathcal{T}}, \ldots, \mathbf{a}_N^{\mathcal{T}}]^{\mathcal{T}} \in \mathbb{C}^{N \times M}$.

Step 2. Perform permutation to obtain higher gain based on the criteria given in (29). For $n = 1, \ldots, N$, let $\pi_n : \{1, \ldots, M\} \rightarrow \{1, \ldots, M\}$ denote the permutation mapping of dimension n. Namely, $\pi_n(\mathbf{a}_n)$ is the permutation operation of $\mathcal{A}_M$ at nth dimension. Then the N-dimensional constellation can be obtained as

$$\mathcal{C}_{MC} = \left[\pi_1 \left(\mathbf{a}_1^{\mathcal{T}} \right), \pi_2 \left(\mathbf{a}_2^{\mathcal{T}} \right), \ldots, \pi_N \left(\mathbf{a}_N^{\mathcal{T}} \right) \right]^{\mathcal{T}}. \quad (42)$$

The construction of an N-dimensional constellation is equivalent to finding the N permutations $\pi_n, n = 1, 2, \ldots, N$, which can be efficiently solved by using the binary switching algorithm (BSA) [37], [38].

Step 3. Dimension switching. Note that different from conventional codebook design [20], where a basic one-dimensional constellation is repeated at each MC, $\mathcal{C}_{MC}$ is directly designed based on GAM, which introduces inherent power difference among the N dimensions. For the nth dimension, the total energy can be obtained as

$$E_n = c_{\text{norm}}^2 M \left(\xi + n + N \left(\frac{M}{2} - 1 \right) \right), \quad (43)$$

and the power difference between two consecutive dimensions is $E_{n+1} - E_n = c_{\text{norm}}^2 M, 1 \leq n \leq N - 1$. To further maintain the power difference of the sparse codebooks, dimension switching is introduced to $\mathcal{C}_{MC}$ for some users. Specifically, let $\mathbf{c}_n \in \mathbb{C}^{1 \times M}$ be the nth row of $\mathcal{C}_{MC}$, the switched $\mathcal{C}_{MC}$ can be written as

$$\mathcal{C}'_{MC} = \left[\mathbf{c}_N^{\mathcal{T}}, \mathbf{c}_{N-1}^{\mathcal{T}}, \ldots, \mathbf{c}_1^{\mathcal{T}} \right]^{\mathcal{T}}. \quad (44)$$

Remark 5: The major differences between the proposed E-GAM and [19] are: (1) The proposed E-GAM can avoid complex mapping from the GAM points to MC through mapping table; (2) A mathematical design criteria is considered in the proposed E-GAM, which is missing in [19]; (3) A novel dimension switching scheme is further proposed to improve the power diversity.

2) Generate users' sparse codebooks: Based on the $\mathcal{C}_{MC}$ and $\mathcal{C}'_{MC}$, user j's sparse codebook is obtained as

$$\mathcal{X}_j = \begin{cases} \mathbf{V}_j \mathbf{R}_j \mathcal{C}_{MC}, & j \text{ is odd}, \\ \mathbf{V}_j \mathbf{R}_j \mathcal{C}'_{MC}, & j \text{ is even}. \end{cases} \quad (45)$$

(45) introduces row-based energy difference in (41) by $E_1 \neq E_2$, which is useful for improving the distance profile of the superimposed codewords. For example, according to (41), users 2, 3, and 5 superimpose over the first resource node with individual energy of E_2, E_1, and E_1, respectively.

The MC parameters, i.e., ξ, ψ, and the rotation angle $\theta_i, i = 1, 2, \ldots, d_f$ should be optimized according to (27). Let $\mathbf{\Theta} = \left[\theta_1, \theta_2, \ldots, \theta_{d_f}, \xi, \psi \right]^{\mathcal{T}}$ denote all the parameters to be optimized. Based on the proposed MC and constellation superposition scheme, the optimization problem $\mathcal{P}_{1-1}$ is reformulated as

$$\mathcal{P}_{1-2} : \mathcal{X} = \arg\max_{\mathbf{\Theta}} \quad v_{\text{Obj}}(\mathbf{\Theta}) = \mathcal{I}_{LB}^{\mathcal{X}}$$

$$\text{Subject to} \quad v_i(\mathbf{\Theta}) = \begin{cases} -\theta_i \leq 0 \\ \theta_i - \pi \leq 0, i = 1, 2, \ldots, d_f \end{cases}$$

$$v_{d_f+1}(\mathbf{\Theta}) = \begin{cases} -\frac{M}{2} - \xi \leq 0 \\ \xi - \frac{M}{2} \leq 0 \end{cases}$$

$$v_{d_f+2}(\mathbf{\Theta}) = \begin{cases} -\frac{\pi}{M} - \psi \leq 0 \\ \psi - \frac{\pi}{M} \leq 0. \end{cases} \quad (46)$$

Obviously, there are $d_f + 2$ parameters to be optimized in (46). Unfortunately, $v_{\text{Obj}}(\mathbf{\Theta})$ is a non-convex function and the computation complexity of $v_{\text{Obj}}(\mathbf{\Theta})$ is also high, especially for $8 \leq M$. To solve (46), we propose a sample based primal-dual IPM with random initial values. We first transform (46) into a standard barrier problem with the perturbed Karush–Kuhn–Tucker conditions given by [39]

$$\nabla v_{\text{Obj}}(\mathbf{\Theta}) + \sum_{p=1}^{d_f+2} u_p \nabla v_p(\mathbf{\Theta}) = 0,$$
$$u_p \nabla v_p(\mathbf{\Theta}) = -1/t,$$
$$v_p(\mathbf{\Theta}) \leq 0, u_p \geq 0, \quad (47)$$
$$p = 1, 2, \ldots, d_f + 2,$$

where u is the Lagrangian factor and t is the barrier factor. In each iteration, the primal-dual update direction $\Delta\mathbf{\Theta}, \Delta\mathbf{u}$ are obtained by iteration solving the following equation

$$\begin{bmatrix} \mathbf{H}_{\text{es}} & \nabla v(\mathbf{\Theta}) \\ -\text{diag}(\mathbf{u})\nabla v(\mathbf{\Theta}) & -\text{diag}(\mathbf{v}(\mathbf{\Theta})) \end{bmatrix} \begin{bmatrix} \Delta\mathbf{\Theta} \\ \Delta\mathbf{u} \end{bmatrix} = -\begin{bmatrix} \mathbf{r}_{\text{dul}} \\ \mathbf{r}_{\text{cent}} \end{bmatrix}, \quad (48)$$

Algorithm 2 AMI-CB design based on the AMI lower bound $\mathcal{I}_{LB}^{\boldsymbol{\mathcal{X}}}$

Input: J, K, $\mathbf{V}_j$, M, N_0

1: **for** $i_1 = 1 : I_1$ **do**
2:     Randomly choose an initial value of $\boldsymbol{\Theta}$ that satisfies the constraint.
3:     **for** $i_2 = 1 : I_2$ **do**
4:         For the given $\xi, \psi \in \boldsymbol{\Theta}$, generate $\boldsymbol{\mathcal{C}}_{MC}$ based on **Algorithm 1**.
5:         Perform dimension switching and generate $\boldsymbol{\mathcal{X}}_j$ according to (45).
6:         Compute (48) with the proposed sub-optimal estimation, and obtain the update direction $\Delta\boldsymbol{\Theta}, \Delta\mathbf{u}$.
7:         Line search method to determine the update factor ς by minimizing $\|\mathbf{r}_{\text{dul}}\| + \|\mathbf{r}_{\text{cent}}\|$, and then update $\boldsymbol{\Theta} = \Delta\boldsymbol{\Theta} + \varsigma\Delta\boldsymbol{\Theta}$, $\mathbf{u} = \mathbf{u} + \varsigma\Delta\mathbf{u}$.
8:     **end for**
9:     Preserve the current results of $\boldsymbol{\Theta}$ and $v_{\text{Obj}}(\boldsymbol{\Theta})$.
10: **end for**
11: Choose the best result $\boldsymbol{\Theta}^*$ that has the maximum value of $v_{\text{Obj}}(\boldsymbol{\Theta}^*)$, and generate $\boldsymbol{\mathcal{X}}_j$ based on $\boldsymbol{\Theta}^*$.
12: Perform the bit labeling for $\boldsymbol{\mathcal{X}}_j$ based on the criteria given in (30).

---

where $\mathbf{u} = [u_1, u_2, \dots, u_{d_f+2}]^{\mathcal{T}}$, $\mathbf{H}_{\text{es}} = \nabla^2 v_{\text{Obj}}(\boldsymbol{\Theta}) + \sum_{p=1}^{d_f+2} u_p \nabla^2 v_p(\boldsymbol{\Theta})$ is the Hessian matrix, $\mathbf{r}_{\text{dul}} = \nabla v_{\text{Obj}}(\boldsymbol{\Theta}) + \sum_{p=1}^{d_f+2} u_p \nabla v_p(\boldsymbol{\Theta})$, and $\mathbf{r}_{\text{cent}} = -\text{diag}(\mathbf{u})v(\boldsymbol{\Theta}) - 1/t$. In (48), the estimation of $\mathbf{H}_{\text{es}}$ is updated with the BFGS method [39], i.e.,

$$\mathbf{H}_{\text{es}}^{(t+1)} = \mathbf{H}_{\text{es}}^{(t)} + \frac{\mathbf{q}^{(t)}\mathbf{q}^{(t)T}}{\mathbf{q}^{(t)}\Delta\boldsymbol{\Theta}^{(t)}} - \frac{\mathbf{H}_{\text{es}}^{\mathcal{T}}\Delta\boldsymbol{\Theta}^{(t)}\Delta\boldsymbol{\Theta}^{(t)T}\mathbf{H}_{\text{es}}^{(t)T}}{\Delta\boldsymbol{\Theta}^{(t)T}\mathbf{H}_{\text{es}}^{(t)}\Delta\boldsymbol{\Theta}^{(t)}}, \quad (49)$$

where $\mathbf{q}^{(t)} = \sum_{p=1}^{d_f+2} u_p \left(\nabla v_p(\boldsymbol{\Theta}^{(t+1)}) - \nabla v_p(\boldsymbol{\Theta}^{(t)})\right) + \nabla v_{\text{Obj}}(\boldsymbol{\Theta}^{(t+1)}) - \nabla v_{\text{Obj}}(\boldsymbol{\Theta}^{(t)})$. The above iteration stops when the size of the current step is less than the value of the step size tolerance or the constraints are satisfied to within the value of the constraint tolerance. Since the $\mathcal{I}_{LB}^{\boldsymbol{\mathcal{X}}}$ is a non-differentiable function, the difference method is employed to calculate the numerical gradient $\nabla v_{\text{Obj}}(\boldsymbol{\Theta})$. Due to the high computational complexity of calculating $\nabla v_{\text{Obj}}(\boldsymbol{\Theta})$ for $M \geq 8$, a sub-optimal Monte Carlo sample of $\nabla v_{\text{Obj}}(\boldsymbol{\Theta})$ for $M \geq 8$ is used to estimate its true value. In addition, due to the non-convex of the objection function, the above process can be performed several times with different initial conditions to prevent it from converging into local optimum. The overall proposed efficient codebook design based on the AMI lower bound is summarized in Algorithm 2.

3) Perform bit labeling: For each of the sparse codebook $\boldsymbol{\mathcal{X}}_j$, we only construct its M codewords for the codebook, the corresponding bit-to-symbol mapping, i.e., bit labeling, is further need to be assigned. For an M-ary codebook, there are a total of $T = M!$ labeling methods. The BSA can be employed again to find the labeling solution for $M \geq 8$ with reasonable complexity, whereas the labeling can be done by exhaustive search for the codebook set with small M, i.e.,

---

Algorithm 3 P-CB design based on the PEP upper bound in (24)

Input: J, K, $\mathbf{V}_j$, M, N_0

1: For given M, choose a one-dimensional basic constellation $\mathbf{a}$ from the constellation pool.
2: Permute $\mathbf{p}$ to obtain $\boldsymbol{\mathcal{C}}_{MC}$ according to the criteria given in (36).
3: From the perspective of the basic constellation $\mathbf{p}$, obtaining the optimal rotation angles $\theta_{\text{opt}}^1 \in (0, \frac{\pi}{2}]$ and $\theta_{\text{opt}}^2 \in (-\frac{\pi}{2}, 0]$ that achieve the largest DO and MMPD, and let $\theta_1 = \theta_{\text{opt}}^1$, $\theta_2 = \theta_{\text{opt}}^2$.
4: From the perspective of the superimposed codewords, search $\theta_3 \in [-\pi, \pi]$ for the largest $\tau_{\text{min}}^{\boldsymbol{\mathcal{X}}}$ in (52).
5: According to (41), generate sparse codebooks by $\boldsymbol{\mathcal{X}}_j = \mathbf{V}_j\mathbf{R}_j\boldsymbol{\mathcal{C}}_{MC}, j = 1, 2, \dots, J$.
6: Perform bit labeling for the optimized codebook $\boldsymbol{\mathcal{X}}_j$, and use the labeling metric given in (37).

$M \leq 4$.

C. Design of P-CB

1) Design of $\boldsymbol{\mathcal{C}}_{MC}$: In contrast to the case for the AMI based MC design, a MC with large MPD, i.e, $d_{\text{MPD}}^{\boldsymbol{\mathcal{C}}_{MC}}$, is required for the PEP based design. To this end, we first choose a one-dimensional basic constellation with large MED, denoted as $\mathbf{p}$, and then permute $\mathbf{p}$ to obtain $\boldsymbol{\mathcal{C}}_{MC}$. Namely, the N-dimensional constellation can be obtained as

$$\boldsymbol{\mathcal{C}}_{MC} = [\pi_1(\mathbf{p}), \pi_2(\mathbf{p}), \dots, \pi_N(\mathbf{p})]^{\mathcal{T}}. \quad (50)$$

Similar to the AMI based codebook design, the permutation is obtained by performing BSA according to the criteria given in (36).

2) Generate sparse codebooks: Multiple sparse codebooks are generated by $\boldsymbol{\mathcal{X}}_j = \mathbf{V}_j\mathbf{R}_j\boldsymbol{\mathcal{C}}_{MC}$ based on the signature matrix given in (41). Let p_i denote the ith signal point in $\mathbf{p}$. Based on (41), the superimposed constellation on a resource node can be obtained by

$$\boldsymbol{\mathcal{S}}_{\text{sum}} = \left\{ p_i^{(1)}e^{j\theta_1} + p_i^{(2)}e^{j\theta_2} + \dots + p_i^{(d_f)}e^{j\theta_{d_f}} \right.$$
$$\left. |\forall p_i^{(l)} \in \mathbf{p}, l = 1, 2, \dots, d_f \right\}. \quad (51)$$

Accordingly, the $\tau_{\text{min}}^{\boldsymbol{\mathcal{X}}}$ in (34) can be simplified to

$$\tau_{\text{min}}^{\boldsymbol{\mathcal{X}}} = \min_{m \neq n} \left\{ \min \left\{ |\mathfrak{Re}(s_m - s_n)|^2, |\mathfrak{Im}(s_m - s_n)|^2 \right\} \right\}, \quad (52)$$

where s_m is the mth point of $\boldsymbol{\mathcal{S}}_{\text{sum}}$. According to (35), the rotation angles, i.e., $\boldsymbol{\theta} = [\theta_1.\theta_2, \dots, \theta_{d_f}]$, should be designed to achieve full DO, large MMPD $(d_{\text{P,min}}^{\boldsymbol{\mathcal{X}}})$, and large $\tau_{\text{min}}^{\boldsymbol{\mathcal{X}}}$, i.e.,

$$\mathcal{P}_{2-2} : \boldsymbol{\theta}^* = \arg\max_{\boldsymbol{\theta}} \left\{ d_{\text{MMPD}}^{\boldsymbol{\mathcal{X}}}, \tau_{\text{min}}^{\boldsymbol{\mathcal{X}}} \right\}$$
$$\text{Subject to} \quad (35a). \quad (53)$$

Unfortunately, there is no optimal solution for (53). This is because once the sparse codebook $\boldsymbol{\mathcal{X}}_j$ with full DO and optimal MMPD is achieved, $\mathbf{R}_j$ is determined, indicating there is no degree of freedom to improve $\tau_{\text{min}}^{\boldsymbol{\mathcal{X}}}$. However, as mentioned, it is ideal to maximize the DO and MMPD

first and then improve $\tau^{\boldsymbol{\mathcal{X}}}_{\min}$. Hence, we consider a feasible way by transforming (53) into a multi-stage design problem. Specifically, the optimal rotation angles that achieve full DO and optimal MMPD of **p** are first obtained. Then, the rest of angles are determined by maximizing $\tau^{\boldsymbol{\mathcal{X}}}_{\min}$. The detailed design process is summarized in **Algorithm 3**.

3) Perform bit labeling: Similar to the AMI based labeling scheme, bit labeling is performed according to the metric given in (37).

VI. NUMERICAL RESULTS

In this section, we conduct numerical evaluations of the proposed SSD-SCMA in both uncoded and coded systems with various codebooks. We first evaluate the computational complexity of the proposed codebook design scheme in Subsection VI-A. Then, Subsection VI-B compares the proposed PEP upper bound with the exact ABER, and the AMI lower bound with the exact AMI. Then, the proposed AMI-CBs and P-CBs are presented in Subsection VI-C. Accordingly, with the proposed codebooks, we evaluate the BER performance of SSD-SCMA and C-SCMA in both uncoded and BICM-IDD systems in Subsection VI-D. The indicator matrix that presented in Fig. 1 with $K = 4$, $J = 6$ and $\lambda = 150\%$ is employed. For comparison, we consider the original GAM (OGAM) codebook [19], StarQAM codebook [18], Chen's codebook [20] [2], Huang's codebook [23] and Jiang's codebook [28]. This is because all these codebooks are designed for downlink channels and achieve good BER performance.

A. Computational Complexity

1) AMI-CB design: As discussed in Subsection III-A, the direct calculation of AMI, i.e., (7) is intractable and often calculated by the tedious Monte Carlo method. In general, at least $N_s = 10^3$ noise and channel samples are required to accurately estimate the AMI and its gradient at each iteration. The resultant the computational complexity for AMI can be approximated as $\mathcal{O}\left(N_s M^{2J}\right)$. In contrast, the computational complexity of the proposed lower bound can be approximated as $\mathcal{O}\left(M^{2J}\right)$, which is significantly smaller than that of AMI. In addition, compared to the codebook design scheme proposed in [28], our proposed lower bound of AMI in Rayleigh fading channels has closed-form expression and with simpler computation of $\mathrm{Log}(\cdot)$ operations.

2) P-CB design: The computational complexity of calculating the MMPD is negligible and the main computational complexities of **Algorithm** 3 are imposed by the operations of permutation, labeling, and the maximizing of $\tau^{\boldsymbol{\mathcal{X}}}_{\min}$. With the aid of BSA algorithm, the computational complexity of permutation and labeling can be reduced to $\mathcal{O}\left(M^2\right)$. In addition, the complexity of determining the θ_3 by maximizing $\tau^{\boldsymbol{\mathcal{X}}}_{\min}$ can be approximated as $\mathcal{O}\left(KM^{d_f}\right)$ [20]. In general, the design complexity of P-CB is relatively smaller than that of AMI-CB.

[2] For $M = 8$, the NS-QAM proposed in [20] is employed.

TABLE I: The proposed P-CBs.

Codebook	Basic constellation	$[\theta_1, \theta_2, \theta_3]$	MMPD
P-CB1	QPSK	$[0.172\pi, -0.172\pi, 0.068\pi]$	0.86
P-CB2	4-TRI	$[0.083\pi, -0.083\pi, 0.336\pi]$	0.50
P-CB3	8-NS-QAM	$[0.072\pi, -0.072\pi, 0.125\pi]$	0.35
P-CB4	8-TRI	$[0.075\pi, -0.075\pi, 0.378\pi]$	0.36

TABLE II: A comparison of $\mathcal{I}^{\boldsymbol{\mathcal{X}}}_{LB}$ with a constant shift at $E_b/N_o = 5$ dB and $E_b/N_o = 12$ dB for $M = 4$ and $M = 8$, respectively.

M	Codebook	C-SCMA	SSD-SCMA
$M = 4$	AMI-CB1	9.16	10.20
	P-CB1	8.89	9.93
	Chen [20]	8.89	9.85
	Jiang [28]	9.13	9.91
$M = 8$	AMI-CB2	14.82	15.54
	P-CB3	14.60	15.18
	Chen [20]	14.58	15.11
	Jiang [28]	14.81	15.30

B. Evaluations of PEP upper bound and AMI lower bound

We now compare the ABER of Chernoff bound with the proposed PEP upper bound in (21) and (26) by employing the StarQAM codebook in SSD-SCMA. As shown in Fig. 4, for $M = 4$, the proposed upper bound, i.e., the line "Prop.", close to the simulated ABER at high SNR, while the Chernoff bound is about 2 dB away from the simulated ABER. For $M = 8$, the Chernoff bound is about 3 dB away the simulated ABER, however, the proposed PEP upper bound still holds very tight to the simulated ABER in high E_b/N_o regime.

As discussed in Subsection III-A, direct calculation of AMI, i.e., (7) is intractable and hence Monte Carlo method is applied. Suppose about N_s noise and channel samples are required to accurately estimate the AMI. Hence the computational complexity can be approximated as $\mathcal{O}\left(N_s M^{2J}\right)$, which may be not affordable for $M \geq 8$. As mentioned in *Remark 2*, there exists a constant gap between the AMI and the proposed lower bound and this can be leveraged for AMI analysis. Fig. 5 shows the AMI obtained by Monte Carlo simulation and the proposed AMI lower bound with a constant shift for both SSD-SCMA and C-SCMA with $M = 4$. One can see that the proposed AMI lower bound plus a constant fits well the simulated AMI over the low and high SNR ranges. For the other middle-range, there exists a small gap between the estimated AMI and the AMI lower bound with a constant shift. However, it is still effective to improve the AMI by maximizing the lower bound.

C. The Proposed Codebooks

1) The proposed P-CBs: We consider the following one dimensional basic constellations **p** employed for the PEP based codebook: quadrature phase shift keying (QPSK), non-square quadrature amplitude modulation (NS-QAM) and the constellation drawn from a lattice of equilateral triangles [40], denoted as M-TRI. The MED of the basic constellation, denoted by $d_{\min}$, is also given. Based on QPSK, 4-TRI, NS-QAM and 8-TRI, the resultant codebooks are respectively
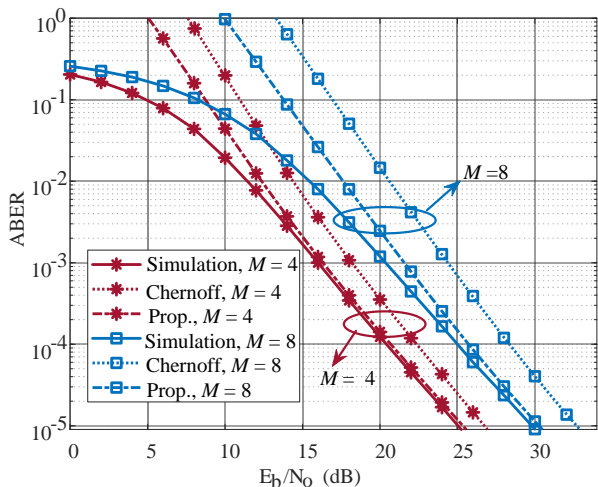
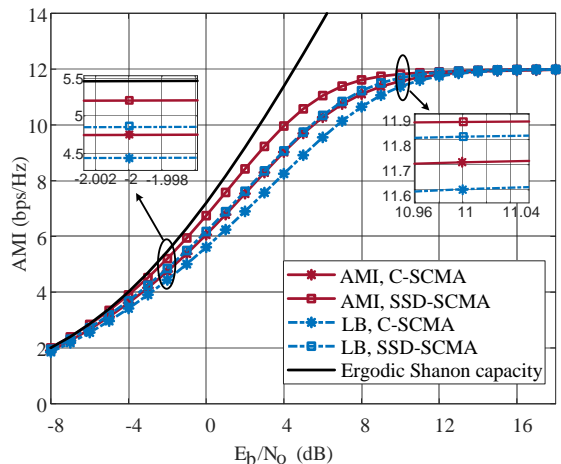Fig. 4: ABER against various upper bounds for SSD-SCMA system.

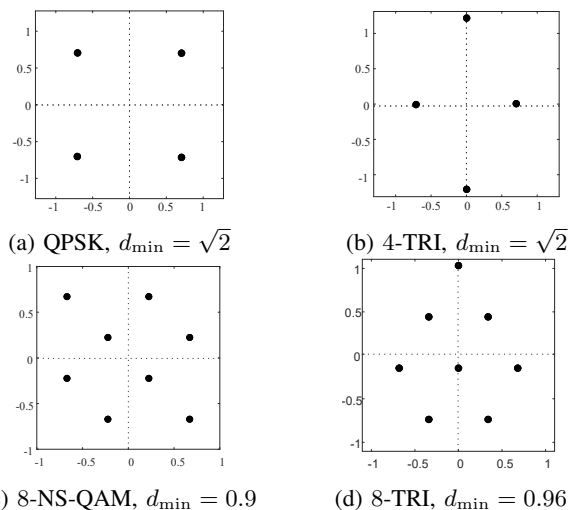Fig. 5: The AMI and the lower bound of AMI for SSD-SCMA and C-SCMA systems.

(a) QPSK, $d_{\min} = \sqrt{2}$

(b) 4-TRI, $d_{\min} = \sqrt{2}$

(c) 8-NS-QAM, $d_{\min} = 0.9$

(d) 8-TRI, $d_{\min} = 0.96$

Fig. 6: The adopted basic one dimensional constellation **p** with large MED ($d_{\min}$). The resultant codebooks are respectively denoted as P-CB1, P-CB2, P-CB3 and P-CB4.

denoted as P-CB1, P-CB2, P-CB3 and P-CB4. The labeling is carried out at $E_b/N_o = 15$ dB for both $M = 4$ and $M = 8$. The rotation angles and the MMPDs corresponding to θ_{opt} are also summarized in Table I.

2) The proposed AMI-CBs: In Algorithm 2, we set $I_1 = 10$ and $I_2 = 25$ to generate the AMI-CBs. Table II compares the $\mathcal{I}_{LB}^{\mathcal{X}}$ with a constant shift of $-K(1/\ln 2 - 1)$ for various codebooks. The proposed AMI-CBs own larger value of $\mathcal{I}_{LB}^{\mathcal{X}}$, especially for SSD-SCMA system. As discussed in Section IV-C, a codebook with larger MMPD (MPD) owns larger $\mathcal{I}_{LB}^{\mathcal{X}}$ of SSD-SCMA (conventional SCMA). We now give an example to illustrate this relationship. Consider the C-SCMA system, the MPDs for the proposed P-CB1, Chen's codebook and StarQAM codebook are respectively given as 1, 1 and 0.72, whereas the $\mathcal{I}_{LB}^{\mathcal{X}}$ with a constant shift for those codebooks at $E_b/N_o = 12$ dB are 11.89, 11.89 and 11.78, respectively. However, this may not hold for low and mid

range SNRs, which can been seen in Table II. In general, the asymptotic relationship holds when $E_b/N_o \geq 12$ dB and $E_b/N_o \geq 16$ dB for $M = 4$ and $M = 8$, respectively. The optimized parameters $[\psi, \xi, \theta_1, \theta_2, \theta_3]$ for AMI-CB1 and AMI-CB2 are given as $[-0.525, 0.659, -0.109, 0.272, 0.555]$ and $[-0.452, 0.700, -0.131, 0.152, 0.455]$, respectively. Interested readers can find the proposed AMI-CB1 in Appendix A, and more relevant results at our GitHub project[3].

D. BER performance of the proposed SSD-SCMA

1) Uncoded system: We first evaluate the uncoded BER performance of SSD-SCMA system with P-CBs, as shown in Fig. 7 and Fig. 8. The dash lines denote the BERs for conventional SCMA, whereas the solid lines are the proposed SSD-SCMA. The main observations are summarized as follows:

- The proposed SSD-SCMA outperforms C-SCMA for both $M = 4$ and $M = 8$. For $M = 4$, 5.5 dB can be observed for SSD-SCMA with the proposed P-CB1 over that of C-SCMA with Chen's codebook at BER $= 10^{-5}$, whereas 4 dB gain is achieved for $M = 8$ with the proposed P-CB3. In addition, SSD-SCMA exhibits steeper BER slopes than that of C-SCMA due to the larger DO of the former.

- Not all codebooks can achieve such large gain for SSD-SCMA system. For example, only 2 dB gain is observed for Star-QAM codebook. Interestingly, the proposed SSD-SCMA can improve the BER performance of Huang's codebook by 6 dB. It is noted that the advantage of Huang's codebook is in Gaussian channels, however, we show that its BER performance is significantly improved with the proposed SSD-SCMA over Rayleigh fading channels.

- The proposed P-CB1 and PCB3 achieve the best BER performance for both SSD-SCMA and C-SCMA systems, owing to the well optimized MPD, MMPD, DO and labeling.
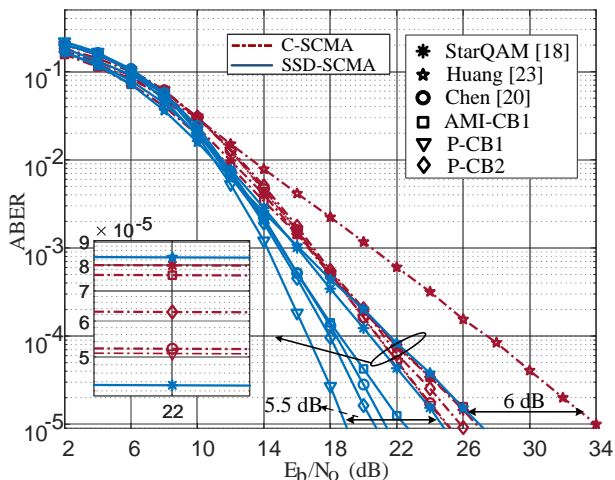
[3]https://github.com/ethanlq/SCMA-codebook

Fig. 7: ABER comparison between SSD-SCMA and C-SCMA systems of various codebooks of $M = 4$.

Fig. 8: ABER comparison between SSD-SCMA and C-SCMA systems of various codebooks of $M = 8$.

Fig. 9: BLER comparison between SSD-SCMA and C-SCMA systems of various codebooks for $M = 4$.
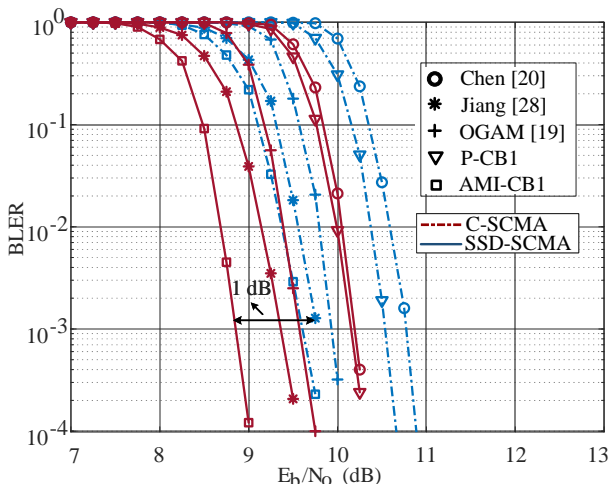

Fig. 10: BLER comparison between SSD-SCMA and C-SCMA systems of various codebooks for $M = 8$.

2) BICM-IDD system: Next, we evaluate the BER performance of coded SSD-SCMA with AMI-CBs under BICM-IDD receiver structure. Specifically, the 5G NR LDPC code, as specified in TS38.212 [41], with block length of 1024 and rate of $5/6$ are considered. The Eb/No for optimizing a codebook is determined according to the code rate [9]. Specifically, the Eb/No that achieves an AMI of $rJ \log(M)$ is considered, where r denotes the code rate. Namely, for a code rate of $5/6$, we employ the codebooks of $M = 4$ and $M = 8$ that are optimized at Eb/No $= 4$ dB and Eb/No $= 12$ dB, respectively. The number of MPA iterations is 3, the maximum number of LDPC decoding iterations is 25 and the number of BICM-IDD iterations is 4.

Fig. 9 and Fig. 10 show the block error rate (BLER) performances of various codebooks for $M = 4$ and $M = 8$, respectively. The main observations are summarized as follows:

- The proposed SSD-SCMA with the proposed AMI-CBs achieve the best BLER performance among all bench-
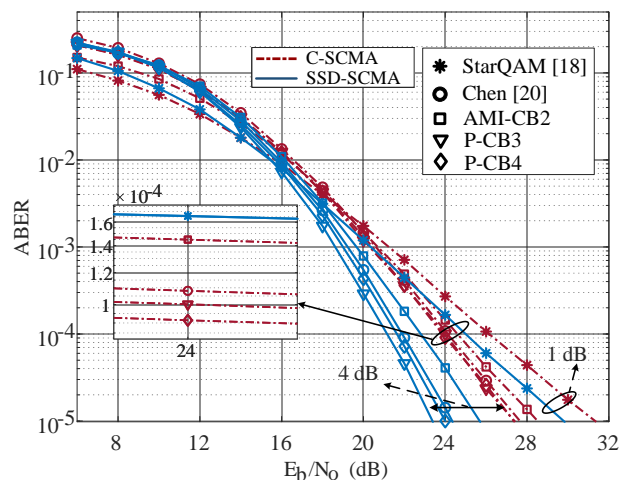
marking codebooks due to its optimized AMI and labeling. Specifically, the proposed SSD-SCMA with AMI-CB1 and AMI-CB2 can achieve about 1 dB and 0.75 dB gains compared to C-SCMA with the StarQAM codebook for $M = 4$ and $M = 8$, respectively.

- It is worth mentioning that a codebook that achieves better BER performance in an uncoded system may not outperform in a BICM-IDD system, and vice versa. For example, the proposed PCB1 and Chen' codebook achieve better BER performance than the Star-QAM, OGAM codebooks and the proposed AMI-CB1 in uncoded C-SCMA with $M = 4$; however, their error performances deteriorate under the BICM-IDD system. This is because their performance metrics and codebook design criteria are different from each other.

VII. CONCLUSIONS

In this paper, we have introduced a novel SSD-SCMA that can significantly improve the error performance of SCMA in

downlink Rayleigh fading channels. We have analyzed the AMI and PEP of SSD-SCMA, and derived the AMI lower bound and PEP upper bound. Based on the proposed bounds, a systematic codebook design metrics have been established for both AMI-CBs and P-CBs. The asymptotic relationship between the two codebook designs based on PEP and AMI have been revealed. Furthermore, a novel E-GAM has been proposed as the MC to design the AMI-CBs, whereas an efficient approach by permuting a basic constellation has been introduced to design P-CBs. Numerical results have demonstrated the advantages of the proposed SSD-SCMA with the proposed AMI-CBs and P-CBs in both uncoded and BICM-IDD systems.

APPENDIX A
THE PROPOSED CODEBOOKS

The proposed AMI-CB1 is presented, and the other codebooks can be constructed with the presented parameters. Alternatively, one can find these codebooks at: https://github.com/ethanlq/SCMA-codebook. For $M = 4$, the four columns of $\mathcal{X}_j, j = 1, 2, \ldots, J$ denote the codewords labelled by 00, 01, 10, 11, respectively.

$$\mathcal{X}_1 = \begin{bmatrix} 0 & 0.0432 - 0.7904i & 0 & -0.5417 - 0.2827i \\ 0 & -0.1541 - 0.3106i & 0 & 0.5097 + 0.7873i \\ 0 & 0.1541 + 0.3106i & 0 & -0.5097 - 0.7873i \\ 0 & -0.0432 + 0.7904i & 0 & 0.5417 + 0.2827i \end{bmatrix}^{\mathcal{T}},$$

$$\mathcal{X}_2 = \begin{bmatrix} 0.3884 - 0.4718i & 0 & 0.0432 - 0.7904i & 0 \\ -0.8755 + 0.3364i & 0 & -0.1541 - 0.3106i & 0 \\ 0.8755 - 0.3364i & 0 & 0.1541 + 0.3106i & 0 \\ -0.3884 + 0.4718i & 0 & -0.0432 + 0.7904i & 0 \end{bmatrix}^{\mathcal{T}},$$

$$\mathcal{X}_3 = \begin{bmatrix} -0.5853 - 0.5329i & 0.3884 - 0.4718i & 0 & 0 \\ -0.3382 - 0.0768i & -0.8755 + 0.3364i & 0 & 0 \\ 0.3382 + 0.0768i & 0.8755 - 0.3364i & 0 & 0 \\ 0.5853 + 0.5329i & -0.3884 + 0.4718i & 0 & 0 \end{bmatrix}^{\mathcal{T}},$$

$$\mathcal{X}_4 = \begin{bmatrix} 0 & 0 & -0.5417 - 0.2827i & 0.0432 - 0.7904i \\ 0 & 0 & 0.5097 + 0.7873i & -0.1541 - 0.3106i \\ 0 & 0 & -0.5097 - 0.7873i & 0.1541 + 0.3106i \\ 0 & 0 & 0.5417 + 0.2827i & -0.0432 + 0.7904i \end{bmatrix}^{\mathcal{T}},$$

$$\mathcal{X}_5 = \begin{bmatrix} 0.0432 - 0.7904i & 0 & 0.3884 - 0.4718i \\ -0.1541 - 0.3106i & 0 & 0 & -0.8755 + 0.3364i \\ 0.1541 + 0.3106i & 0 & 0 & 0.8755 - 0.3364i \\ -0.0432 + 0.7904i & 0 & 0 & -0.3884 + 0.4718i \end{bmatrix}^{\mathcal{T}},$$

$$\mathcal{X}_6 = \begin{bmatrix} 0 & -0.5417 - 0.2827i & 0.6422 - 0.4628i & 0 \\ 0 & 0.5097 + 0.7873i & 0.1449 - 0.3150i & 0 \\ 0 & -0.5097 - 0.7873i & -0.1449 + 0.3150i & 0 \\ 0 & 0.5417 + 0.2827i & -0.6422 + 0.4628i & 0 \end{bmatrix}^{\mathcal{T}}.$$

REFERENCES

[1] Z. Liu and L.-L. Yang, "Sparse or dense: A comparative study of code-domain NOMA systems," *IEEE Trans. Wireless Commun.*, vol. 20, no. 8, pp. 4768–4780, Aug. 2021.
[2] Q. Luo, Z. Mheich, G. Chen, P. Xiao, and Z. Liu, "Reinforcement learning aided link adaptation for downlink NOMA systems with channel imperfections," in *IEEE WCNC*. Glasgow, U.K.: IEEE, Mar. 2023.
[3] H. Nikopour and H. Baligh, "Sparse code multiple access," in *Proc. IEEE 24th Int.Symp. Pers., Indoor, Mobile Radio Commun. (PIMRC)*, London, U.K., Sep. 2013, pp. 332–336.
[4] M. Taherzadeh, H. Nikopour, A. Bayesteh, and H. Baligh, "SCMA codebook design," in *Proc. IEEE 80th Veh. Techno. Conf. (VTC2014-Fall)*, Vancouver, Canada, Dec. 2014, pp. 1–5.
[5] Q. Luo, Z. Liu, G. Chen, Y. Ma, and P. Xiao, "A novel multitask learning empowered codebook design for downlink SCMA networks," *IEEE Wireless Commun. Lett.*, vol. 11, no. 6, pp. 1268–1272, 2022.
[6] J. Boutros and E. Viterbo, "Signal space diversity: a power- and bandwidth-efficient diversity technique for the Rayleigh fading channel," *IEEE Trans. Inf. Theory*, vol. 44, no. 4, pp. 1453–1467, Jul. 1998.
[7] M. N. Khormuji, U. H. Rizvi, G. J. Janssen, and S. B. Slimane, "Rotation optimization for MPSK/MQAM signal constellations over Rayleigh fading channels," in *IEEE ICC workshop*. Singapore: IEEE, 2006, pp. 1–5.
[8] S. Jeon, I. Kyung, and M.-S. Kim, "Component-interleaved receive mrc with rotated constellation for signal space diversity," in *IEEE 70th VTC Fall*, Anchorage, USA, Sep. 2009, pp. 1–6.
[9] Q. Xie, J. Song, K. Peng, F. Yang, and Z. Wang, "Coded modulation with signal space diversity," *IEEE Trans. Wireless Commun.*, vol. 10, no. 2, pp. 660–669, Feb. 2011.
[10] A. Chindapol and J. Ritcey, "Design, analysis, and performance evaluation for BICM-ID with square QAM constellations in Rayleigh fading channels," *IEEE J. Sel. Areas Commun.*, vol. 19, no. 5, pp. 944–957, May 2001.
[11] J. C. Inácio, B. F. Uchôa-Filho, D. Le Ruyet, and S. Montejo-Sánchez, "Full diversity multidimensional codebook design for fading channels: The combinatorial approach," *IEEE Trans. Commun.*, vol. 68, no. 7, pp. 4104–4116, 2020.
[12] J. C. Inácio, B. F. Uchôa-Filho, and D. L. Ruyet, "Low-complexity detection for multidimensional codebooks over fading channels," *IEEE Trans. Wireless Commun.*, pp. 1–1, 2022.
[13] M. Qiu, Y.-C. Huang, and J. Yuan, "Downlink non-orthogonal multiple access without SIC for block fading channels: An algebraic rotation approach," *IEEE Trans. Wireless Commun.*, vol. 18, no. 8, pp. 3903–3918, Aug. 2019.
[14] S. Özyurt and O. Kucur, "Quadrature NOMA: A low-complexity multiple access technique with coordinate interleaving," *IEEE Wireless Commun.Lett.*, vol. 9, no. 9, pp. 1452–1456, May 2020.
[15] G. Pandey and A. Jaiswal, "Coordinated and non-coordinated direct-and-relay transmission: A signal space diversity approach," *IEEE Commun. Lett.*, vol. 25, no. 6, pp. 1825–1829, Nov. 2021.
[16] Z. Zhang, Z. Ma, X. Lei, M. Xiao, C.-X. Wang, and P. Fan, "Power domain non-orthogonal transmission for cellular mobile broadcasting: Basic scheme, system design, and coverage performance," *IEEE Wireless Commun.*, vol. 25, no. 2, pp. 90–99, 2018.
[17] B. K. Ng and C.-T. Lam, "Joint power and modulation optimization in two-user non-orthogonal multiple access channels: A minimum error probability approach," *IEEE Trans. Veh. Techno.*, vol. 67, no. 11, pp. 10 693–10 703, 2018.
[18] L. Yu, P. Fan, D. Cai, and Z. Ma, "Design and analysis of SCMA codebook based on Star-QAM signaling constellations," *IEEE Trans. Veh. Technol.*, vol. 67, no. 11, pp. 10 543–10 553, Aug. 2018.
[19] Z. Mheich, L. Wen, P. Xiao, and A. Maaref, "Design of SCMA codebooks based on golden angle modulation," *IEEE Trans. Veh. Technol.*, vol. 68, no. 2, pp. 1501–1509, Dec. 2018.
[20] Y.-M. Chen and J.-W. Chen, "On the design of near-optimal sparse code multiple access codebooks," *IEEE Trans. Commun.*, vol. 68, no. 5, pp. 2950–2962, Feb. 2020.
[21] X. Zhang, D. Zhang, L. Yang, G. Han, H.-H. Chen, and D. Zhang, "SCMA codebook design based on uniquely decomposable constellation groups," *IEEE Trans. Wireless Commun.*, vol. 20, no. 8, pp. 4828–4842, Mar. 2021.
[22] Q. Luo, Z. Liu, G. Chen, P. Xiao, Y. Ma, and A. Maaref, "A design of low-projection SCMA codebooks for ultra-low decoding complexity in downlink IoT networks," *IEEE Trans. Wireless Commun.*, 2023.
[23] C. Huang, B.-C. Su, T. Lin, and Y. Huang, "Downlink SCMA codebook design with low error rate by maximizing minimum Euclidean distance of superimposed codewords," *IEEE Trans. Veh. Technol.*, 2022.
[24] C. Dong, G. Gao, K. Niu, and J. Lin, "An efficient SCMA codebook optimization algorithm based on mutual information maximization," *Wireless Commun. Mobile Comput.*, vol. 2018, 2018.
[25] J. Bao, Z. Ma, Z. Ding, G. K. Karagiannidis, and Z. Zhu, "On the design of multiuser codebooks for uplink SCMA systems," *IEEE Commun. Lett.*, vol. 20, no. 10, pp. 1920–1923, Oct. 2016.
[26] K. Xiao, B. Xia, Z. Chen, B. Xiao, D. Chen, and S. Ma, "On capacity-based codebook design and advanced decoding for sparse code multiple access systems," *IEEE Trans. Wireless Commun.*, vol. 17, no. 6, pp. 3834–3849, June 2018.
[27] S. Sharma, K. Deka, V. Bhatia, and A. Gupta, "SCMA codebook based on optimization of mutual information and shaping gain," in *2018 IEEE Globecom Workshops (GC Wkshps)*, Dec. 2018, pp. 1–6.
[28] C. Jiang, Y. Wang, P. Cheng, and W. Xiang, "A low-complexity codebook optimization scheme for sparse code multiple access," *IEEE Trans. Commun.*, vol. 70, no. 4, pp. 2451–2463, 2022.
[29] Y. Yao, K. Xiao, B. Xia, and Q. Gu, "Design and analysis of rotated-QAM based probabilistic shaping scheme for Rayleigh fading channels," *IEEE Trans. Wireless Commun.*, vol. 19, no. 5, pp. 3047–3063, 2020.

[30] Q. Luo, P. Gao, Z. Liu, L. Xiao, Z. Mheich, P. Xiao, and A. Maaref, "An error rate comparison of power domain non-orthogonal multiple access and sparse code multiple access," *IEEE Open J. Commun. Society*, vol. 2, pp. 500–511, 2021.

[31] P. Yang and H. Yang, "A low-complexity linear precoding for MIMO channels with finite constellation inputs," *IEEE Wireless Commun. Lett.*, vol. 8, no. 5, pp. 1415–1418, Oct. 2019.

[32] I. S. Gradshteyn and I. M. Ryzhik, *Table of integrals, series, and products*. Academic press, 2014.

[33] J. Boutros, E. Viterbo, C. Rastello, and J.-C. Belfiore, "Good lattice constellations for both Rayleigh fading and Gaussian channels," *IEEE Trans. Inf. Theory*, vol. 42, no. 2, pp. 502–518, 1996.

[34] G. Taricco and E. Viterbo, "Performance of high-diversity multidimensional constellations," *IEEE Trans. Inf. Theory*, vol. 44, no. 4, pp. 1539–1543, 1998.

[35] Y. Xin, Z. Wang, and G. B. Giannakis, "Space-time diversity systems based on linear constellation precoding," *IEEE Trans. Wireless Commun.*, vol. 2, no. 2, pp. 294–309, Mar. 2003.

[36] Z. Yang, Q. Xie, K. Peng, and J. Song, "Labeling optimization for BICM-ID systems," *IEEE Commun. Lett.*, vol. 14, no. 11, pp. 1047–1049, Nov. 2010.

[37] J. Bao, Z. Ma, M. Xiao, T. A. Tsiftsis, and Z. Zhu, "Bit-interleaved coded SCMA with iterative multiuser detection: Multidimensional constellations design," *IEEE Trans. Commun.*, vol. 66, no. 11, pp. 5292–5304, Mar. 2017.

[38] K. Zeger and A. Gersho, "Pseudo-Gray coding," *IEEE Trans. commun.*, vol. 38, no. 12, pp. 2147–2158, Dec. 1990.

[39] S. Boyd, S. P. Boyd, and L. Vandenberghe, *Convex optimization*. Cambridge university press, 2004.

[40] W. Su and X.-G. Xia, "Signal constellations for quasi-orthogonal space-time block codes with full diversity," *IEEE Trans. Info. Theory*, vol. 50, no. 10, pp. 2331–2347, Sep. 2004.

[41] 3GPP TS 38.212, Rel. 15 , "5G NR, multiplexing and channel coding," Jul. 2018. [Online]. Available: https://www.etsi.org/deliver/etsits/138200138299/138212/15.02.0060/ts138212v150200p.pdf